International Journal of Energy and Water Resources
https://doi.org/10.1007/s42108-024-00298-9

ORIGINAL ARTICLE

Use of response surface methodology and CFD for analysing and optimization of simple-air cooled solar panel

V. Singh[1] · V. Trivedi[1] · V. R. Mishra[2]

Received: 2 May 2024 / Accepted: 20 June 2024
© The Author(s), under exclusive licence to Iranian Society of Environmentalists (IRSEN) and Science and Research Branch, Islamic Azad University 2024

Abstract

Solar panel cooling is very much required to sustain its performance. In contrast, air cooling requires small changes in the design of solar panel and has good feasibility to conversion in the actual model. In this research article, a 100 W solar panel was simulated in ANSYS workbench at various solar flux, atmospheric temperature, and the air flow velocity. The numerical results in the form of contour plots of the temperature indicated that if the solar flux and atmospheric temperature are enhanced then, the module temperature increases but the enhancement in the air flow velocity reduces the module temperature. Secondly, the numerical results of the contour plot of temperature also indicate that the maximum temperature hot spot is seen in the middle part of the solar panel. Furthermore, the data obtained from numerical simulation and model equations has been optimized to determine the optimum setting of input and response variables. The optimization work has been completed by Response Surface Methodology (RSM) in MINITAB 17 software. The optimum values of input variables were determined at the maximum values of the solar panel efficiency and exergy efficiency. The optimum solar flux, atmospheric temperature, and air velocity obtained to be 974 W/m^2, 22 °C and 6 m/s on which responses solar panel temperature 51.22 °C, power output 65 W, solar panel efficiency 0.1588, exergy entering into the system 385 W and exergy efficiency 0.1695. To validate the optimum results of the RSM, an experimental setup has been developed and data has been collected at these optimum settings. Finally, the percentage variation in the responses has been calculated to know the error of the predicted results of RSM and experimental observation.

Keywords Solar panel · Exergy · Thermal analysis · RSM · Optimization

Abbreviations

ETFE	Ethylene tetra fluoro ethylene
EVA	Ethylene vinyl acetate
PET	Polyethylene terephthalate
CFRP	Carbon fibre reinforced plastic
FF	Fill factor
CFD	Computational fluid dynamics
RSM	Response surface methodology
MWCNT	Multi-walled nanotubes

List of symbols

S	Solar flux (W/m^2)
A	Area of solar panels (m^2)
T_a	Atmospheric temperature (K)
T_{Sun}	Sun temperature (K)
T_C	Module temperature (K)
E_R	Exergy reflected (W)
E_{XIN}	Exergy entering into the solar panel (W)
E_{XOUT}	Exergy reached in the atmosphere (W)
E_{XDEST}	Exergy destruction due to irreversibility in the system (W)
E_{Loss}	Exergy loss in the atmosphere (W)
E_{Xcel}	Electrical exergy (W)
hc	Heat transfer coefficient W/m^{2}K
I_{SC}	Short circuit current (A)
V_{OC}	Open circuit voltage (V)
β	Inclination of solar panel from horizontal (°)

✉ V. Singh
vineetpsh@gmail.com

V. Trivedi
vaibhavtrivedi@iftmuniversity.ac.in

V. R. Mishra
vr.mishra@glbitm.ac.in

[1] Department of Mechanical Engineering, School of Engineering and Technology, IFTM University, Moradabad, India

[2] Department of Mechanical Engineering, G L Bajaj Institute of Technology and Management, Greater Noida, India

Published online: 15 July 2024

V	Velocity of air flow over the SAH cover plate (m/s)
Nu	Nusselt number
R_{aL}	Rayleigh number
P	Power output of solar panel (W)
k	Thermal conductivity of the solar panel material (W/m. K)

Symbols

ρ	Density of air (Kg/m^3)
σ	Stefan Boltz's man constant (5.67×10^{-8})
ε	Emissivity of solar panel material
α	Absorptivity or absorption coefficient
r	Reflectivity of the solar panel
τ	Transmissivity of the solar panel material
η	Efficiency of solar panel
η_{EX}	Exergy of solar panel
φ_{EX}	Exergetic efficiency of solar panel

Introduction

The availability of solar energy is abundant in the Asiatic region of the world specially in the Indian continent. The solar energy is free from the pollution and renewable in nature. The main problem is only its conversion into electric energy through heat energy. The solar panel converts the solar energy into electric energy easily but the efficiency of conversion is only 10–15% at optimum temperature (Ceylan et al., 2021; Maleki et al., 2020). The maximum efficiency of the solar panel depends on the temperature but the temperature of the solar panel changes throughout the day. In the summer season of the Indian climate, the atmospheric temperature and solar panel material temperature reach more than 40 and 80 °C which leads to the drastic reduction of the performance of solar panel (Malvoni et al., 2020).

There are two main problems with the performance of the solar panel. The first problem is its lower efficiency which can be increased by changing the metallurgy of the solar cells (Choi et al., 2021). The second problem is its lower performance at the higher temperature which is the major problem and can be reduced by providing the cooling of the solar panel (Shah & Mehta, 2021). The higher temperature of solar panel not only reduces the performance of solar panel but also reduces its life span (Marudaipillai et al., 2020). The number of cooling techniques with various cooling fluids has been investigated numerically and experimentally. The effectiveness of cooling depends on the thermal properties of the cooling fluid (Yadav et al., 2021). Table 1 represents the properties of various cooling fluids used in cooling of solar panel. The data represented in Table 1 obtained from the previously published research.

The air, water, nanomaterial, and phase change materials were the cooling fluids under investigation. The air cooling in natural and forced convection with various types of fins are very effective. A study on solar panel cooling have been conducted for knowing the effect of variation of solar flux, atmospheric temperature, number of fins and fin pitch. The results saw that as the fin pitch increases the number of fins reduces which leads to enhance in the module temperature. If the fin pitch increases from 20 to 60 mm, the PV module temperature increases from 44.13 to 54.01 °C (Elbreki et al., 2020). The forced air cooling with water injection is very effective (Kabeel & Abdelgaied, 2019). Air cooling with the various types of fins, fin spacing and number of fins plays an important role in heat transfer (Mankani et al., 2022). The effect of air mass flow rate increasing the cooling rate of the solar panel since increasing the heat transfer coefficient. As the solar flux increasing from morning to after noon the solar panel temperature also increasing so this increase in temperature has been compensated with increase in mass flow rate (Patil et al., 2023). The air cooling to the solar panel is very economical but the water cooling by spray form gave better results (Sultan et al., 1973). A 60 Wp solar panel has been tested in air cooling, the supply of the air continued upto 15 min (Revati & Natarajan, 2016). The thermal conductivity and specific heat of water are 0.6 W/m K and 4.15 kJ/Kg K as compared to air 0.026 W/m K and 1.015 kJ/Kg K around 23 and 4 times higher than the air. Which shows water is better option than air for removing and storing the heat from the solar panel even the pumping power consumed in water is quite less than the air (Vineet et al., 2023).

A concentrated solar panel enhanced the solar flux intensity on the solar panel surface and maintained the optimum temperature of around 315.15 K by water cooling. This system enhance the thermal and electric efficiency of the solar panel (Chaabane et al., 2016). An indoor study on cooling of solar panel by water has been conducted to investigate the

Table 1 Properties of cooling fluids used in previous published research article (Ebaid et al., 2017; Fayaz et al., 2018; Tian et al., 2021)

S. No.	Properties of the fluid	Air	Water	Nano fluids			
				MWCNT	TiO_2	Al_2O_3	MgO
1	ρ	1.21	997.1	1600	1003.6	1003.43	3580
2	k	0.026	0.613	3000	0.6265	0.6590	54.9
3	C_P	1005	4179	796	–	–	937
4	μ			–	0.000802716	0.000803129	

effect of temperature on solar panel efficiency. The results depicted that the enhancement in the efficiency of the solar panel is more than 35% of the previous efficiency (Peng et al., 2017). A pulsed cooling system has been investigated to maintain the temperature of solar panel for saving water wastage (Hadipour et al., 2021). An ordino-based water cooling system not only reduces the cooling water required but also supplies the water when it is actually required (Laseinde & Ramere, 2021).

A water-cooled solar panel was investigated under varying atmospheric temperature, solar flux and water inlet velocity. The best set of results obtained namely solar flux, water inlet velocity and atmospheric temperature were 705 W/m^2, 0.7263 m/s, and 32.87 °C on which the maximum efficiency of the solar panel was 18.88% (Singh & Yadav, 2022a). A geothermal cooling heat exchanger enhanced the efficiency of solar panel by 9.8% and the electricity generation by 11.2% (Jafari, 2021). A 50 Wp solar panel performance has been improved by providing water cooling on the back side. The test was conducted in Iran and Tehran's climatic conditions. The maximum module temperature of the cooled system was quite high 79.79% as compared with water-cooled solar panel (Shahverdian, 2021). A cooling and power generation combined system has been investigated and optimized by Genetic Algorithm (GA). The Results saw that the maximum thermal and exegetic efficiency were 19.20 and 53.27% (Wang et al., 2020). A hybrid photovoltaic/thermal collector has been investigated for the double benefits of utilising solar energy. The PV/T system is used for producing electrical and thermal energy (Evola & Marletta, 2014). The selection of cooling fluid is very important in case of design of the cooling setup in the solar panel. Table 2 represents the various cooling fluids with their thermal outcomes.

The above literature review focused on the cooling of solar panels by using air, water, PCM, and nanofluids. The effectiveness of the cooling fluid depends on its thermal properties, like thermal conductivity and specific heat. Table 1 represents the comparison of the basic thermal properties of the fluid, and Table 2 represents the various cooling fluid effects on the temperature and efficiency of the solar panel. Except for the air, all liquid fluid cooling techniques require a lot of changes in the design, even if their actual setup is not on the market. Several active and passive methods of air cooling have been proposed, but there is a research gap to identify the optimum selection of the inputs and responses in various environmental conditions. Due to the seasonal variation of the environment, India requires a study that must know the performance of the solar panel in advance. Due to these facts, this research article focused on the thermal analysis of solar panels at various mass flow rates of air. Furthermore, experimental setup, theoretical modeling, optimization technique, ANSYS modeling, results, and discussion and detailed explanation have been presented in the below sections.

Materials and methods

Experimental setup

Figure 1 represents the schematic representation of the cooling of the solar panel. The main components of the experimental setup are a solar panel, fan, pyrometer, Multi thermometer, Anemometer, Digital Multi-meter and thermometer display connector. Table 3 represents the specification of the solar panel and Table 4 represents the specification of the various instruments used for measuring the data at the time of the experimental work. The fan blows the air at varying mass flow rate due to that temperature of the solar panel changed. The solar flux, atmospheric temperature and the air flow velocity is measured by pyrometer, multimeter and anemometer. The three thermocouples have been attached at the top layer of the solar panel and power output from the solar panel has been calculated by determining the current and voltage of the solar panel output. The module temperature is further used for calculating the solar panel efficiency and the exergy efficiency.

Modelling of solar panel

Figure 2a represents the solar panel energy balance. As per the energy balance equation, the total solar energy falling on the surface of the solar panel is reflected, absorbed, and transmitted. So following is the energy balance for the solar panel applied for every layer of the solar panel as shown in Fig. 2b. First, apply the energy balance for the Ethylene Tetra Fluoro Ethylene (ETFE) plate.

Solar Energy on the ETFE plate = Absorption + Reflection + Transmission through the ETFE plate

$$SA = SA\alpha_{ETFE} + SAr_{ETFE} + SA\tau_{ETFE} \tag{1}$$

After further simplification

$$\alpha_{ETFE} + r_{ETFE} + \tau_{ETFE} = 1 \tag{2}$$

The values of absorptivity, reflectivity, and transmissivity of various layers of the solar panel are given in Table 5.

The reflected radiation is the loss of solar energy in the atmosphere and transmitted radiation reaches on the EVA plate but the absorbed radiation by the ETFE plate increases the temperature of the plate.

$$SA\alpha_{ETFE} + Q_{Conduction} - Q_{Convection} - Q_{Radiation} = \frac{mC_P dT_{ETFE}}{dt} \tag{3}$$

Table 2 Various cooling methods of solar panel

S. No.	Author's description	Cooling setup description	Outcomes	Publication year
Natural air cooling				
1	Tonui & Tripanagnostopoulos, 2008)	Air flow duct arrangement on the back side of solar panel with rectangular fins	$\eta_t = 40\%$ $T_{max} = 48\ ^\circ C$	2008
2	Yun et al., 2007)	With the help of solar panel, a ventilated arrangement has been created. This arrangement develops the heating in winter and cooling in summer	$T_{max} = 55.5\ ^\circ C$ (with ventilation) $T_{max} = 76.7\ ^\circ C$ (without ventilation system)	2006
Forced air flow				
1	Teo et al., 2012)	An air duct arrangement has been created at the back of the solar panel	$\eta_E = 12.5\%$ $T_{Max} = 38\ ^\circ C$ $\eta_{E\ Without\ Duct} = 8.5\%$ $T_{Max\ Without\ Duct} = 68\ ^\circ C$	2012
2	Dubey et al., 2009)	A wooden duct has been fixed at the back side of the solar panel and air blown by the 12 V DC produced by the solar panel	$\eta_E = 9.7\%$ $\eta_{E\ Without\ Duct} = 10.41\%$	2009
Water cooling				
1	Royne & Dey, 2007)	The cooling of solar panel has been done by the jet impingement	$\eta_E = 18.01\%$	2007
2	Abdolzadeh & Ameri, 2009)	Made a spray arrangement of water over the 225 Wp solar panel. The test has been conducted to know the overall efficiency of the system	$\eta_O = 12.5\%$	2009
3	He et al., 2006)	A hybrid photovoltaic and thermal collector has been designed and fabricated. The various efficiencies like thermal, electric and overall efficiency has been tested throughout of the day	$\eta_O = 40\%$	2006
4	Zakharchenko et al., 2004)	A PV/T system of a 4 m^2 area has been investigated with a water cooling system. The 90% surface area of the solar panel is contacted by water tubes	The 10% enhancement in the power output of the solar panel	2004
Phase change materials				
1	Chandel & Agarwal, 2017)	_	The 5% efficiency has been increased due to the use of the PCM material	2017
2	Hasan et al., 2014)	Three 65 W solar panel have been used to determine the effect of the PCM material on heat extraction. One panel is considered as the reference panel without PCM material and two solar panels have the PCM material	20 °C temperature drop has been obtained by the use of the PCM material	2014
Nano fluid cooling				
1	Kumar et al., 2020)	Three solar panel have been investigated by simple air, pure water and nano fluid. Two Nano fluids Al_2O_3 and CuO have been used with base fluid water	The maximum temperature drop is obtained at a 0.6% concentration of Al_2O_3 and the maximum efficiency is 12.5%	2020
2	Karami & Rahimi, 2014)	Helical and straight channel cooling effects with Nano fluid have been investigated on solar panel	The results reveal that the maximum electrical efficiency is 20.67 and 37.67%	2014

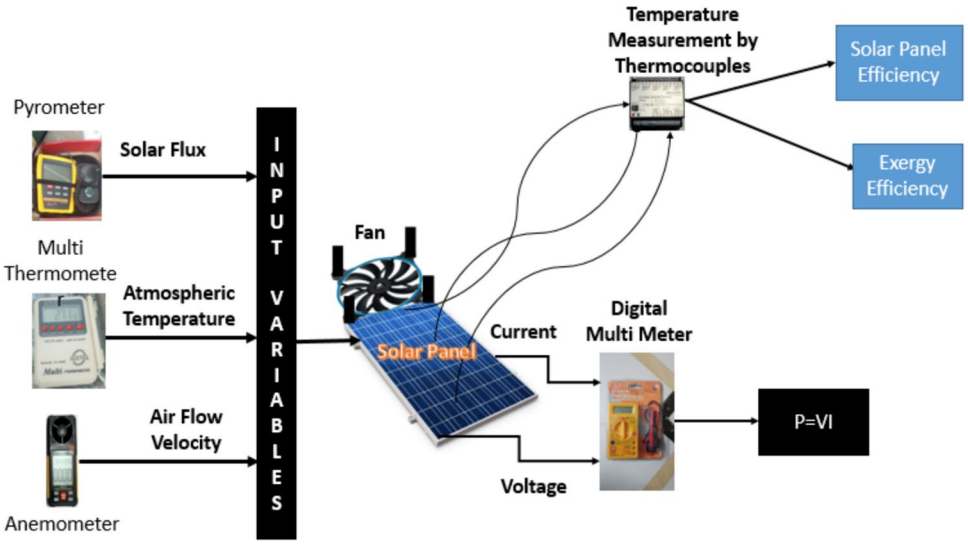

Fig. 1 Schematic representation of experimental setup with the measuring instruments

Table 3 Specification of solar panel

S. No.	Particulate	Numerical Value
1	Irradiance and temperature	1000 W/m^2, AM 1.5 and 25 °C
2	Maximum power	100 W
3	Maximum voltage	18 V
4	Maximum current	5.55 A
5	Open circuit voltage	21.6 V
6	Short circuit current	6.11 A

Table 4 Specification of the instruments

S. No.	Parameter	Instruments	Uncertainty (%)
1	Temperature measurement	Thermocouples	4.25
2	Velocity measurement	Anemometer	4
3	Solar intensity	Pyrometer	4.89
4	Current	Digital multimeter	2.19
5	Voltage	Digital multimeter	3.2

Now apply the energy balance for the silicon solar cell plate

$$SA\tau_{ETFE}\tau_{EVA}\alpha_{Cell} - Q_1 - Q_2 - V_mI_m = \frac{mC_pdT_{Cell}}{dt} \tag{4}$$

The power produced by the solar panel (V_mI_m) has been calculated by the Fill Factor (FF), short circuit current and open circuit voltage by following the formula.

$$FF = \frac{V_mI_m}{I_{SC}V_{OC}} \tag{5}$$

$$V_mI_m = FFI_{SC}V_{OC} \tag{6}$$

The I_{SC} and V_{OC} are the short circuit and open circuit voltage of the solar panel depends on the solar cell material temperature. From the silicon cell in the bottom direction no further radiation transfer occurs since its transmissivity is Zero. The Q_1 and Q_2 amount of heat transfer is takes place from silicon cell from upward and downward directions. In this analysis, it is considered that all layers have been bonded to each other so that convection and radiation heat losses are neglected only heat can be conducted.

The Q1 amount of heat losses from upward direction is given by following relation.

$$Q_1 = \frac{(T_C - T_{atm})}{\left(R1 + R2 + \frac{R_{ConvT}R_{RadT}}{R_{ConvT}+R_{RadT}}\right)} \tag{7}$$

In a similar way heat transfers in the downward direction

$$Q_2 = \frac{(T_C - T_{atm})}{\left(R3 + R4 + R_5 + R_6 + \frac{R_{ConvB}R_{RadB}}{R_{ConvB}+R_{RadB}}\right)} \tag{8}$$

So heat losses from the solar cell in the top and bottom directions are represented by the following equation.

$$Q_{Loss} = Q_1 + Q_2 \tag{9}$$

where R1, R2, R3, R4, R5 and R6 are the conduction resistance of the various layers of the solar panel represented by the following equations.

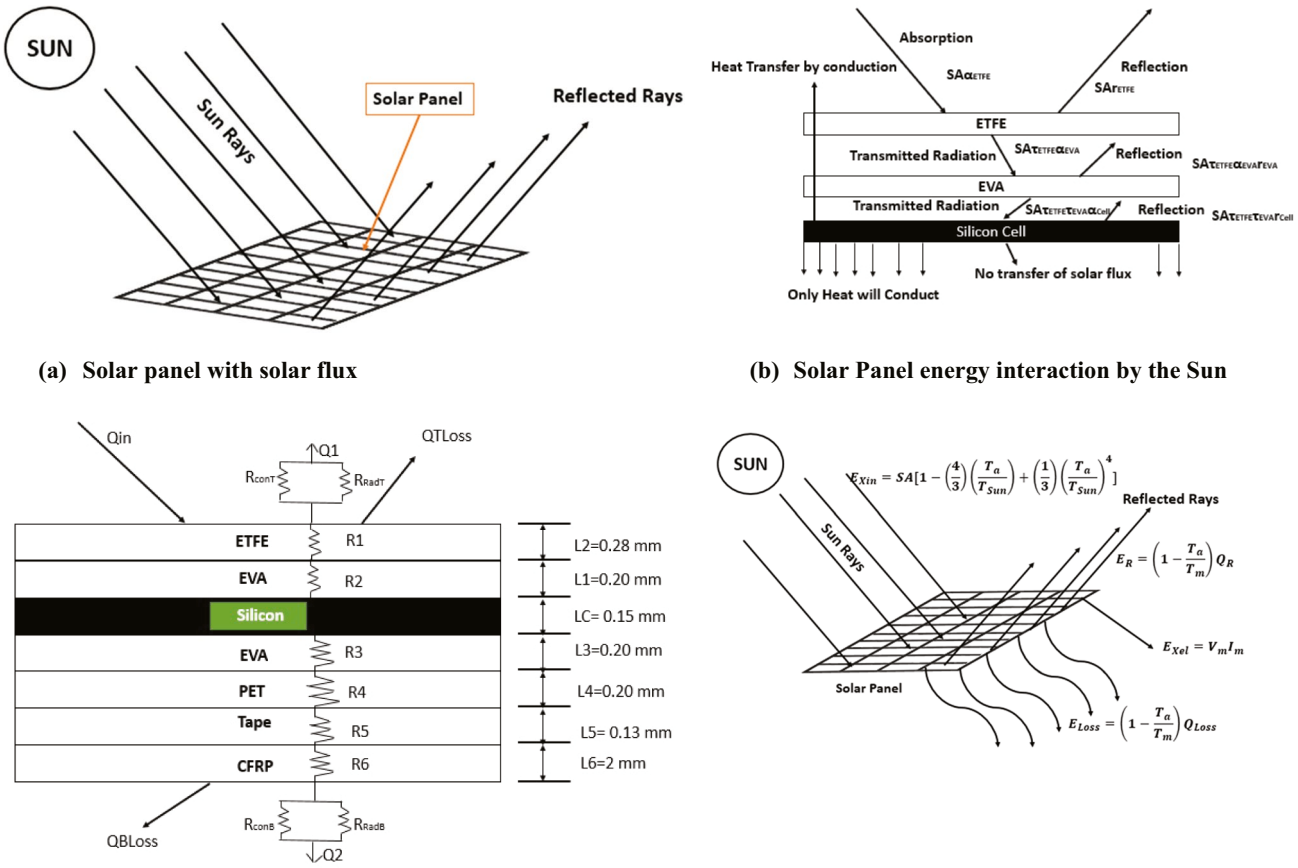

(a) Solar panel with solar flux

(b) Solar Panel energy interaction by the Sun

(c) Heat flow through the solar panel

(d) Exergy flow in solar panel

Fig. 2 Energy balance for the solar panel

Table 5 Optical Properties of solar panel material (Pavlovic et al., 2021)

Material	Absorptivity	Transmissivity	Reflectivity
ETFE	0.1	0.83	0.07
EVA	0	1	0
SI	0.97	0	0.03

Table 6 Thickness and function of various layers of the solar panel material (Pavlovic et al., 2021; Yıldız et al., 2020)

Layer	Function	Material	Thickness (mm)
1	Front sheet	ETFE	0.28
2	Encapsulated	EVA	0.20
3	Solar cell	Silicon	0.15
4	Encapsulated	EVA	0.20
5	Backsheet	PET	0.20
6	Adhesive	Tape	0.13
7	Support	CFRP	2.00

$$R_1 = \frac{L_1}{K_{EVA}A} \tag{10}$$

$$R_2 = \frac{L_2}{K_{ETFE}A} \tag{11}$$

$$R_3 = \frac{L_3}{K_{EVA}A} \tag{12}$$

$$R_4 = \frac{L_4}{K_{PET}A} \tag{13}$$

$$R_5 = \frac{L_5}{K_{Tape}A} \tag{14}$$

$$R_6 = \frac{L_6}{K_{CFRP}A} \tag{15}$$

L_1, L_2, L_3, L_4, L_5 and L_6 are the lengths of EVA, ETFE, EVA, PET, TAPE and CFRP layers of the solar panel represented in Fig. 2c and Table 6. The K_{EVA}, K_{ETFE}, K_{PET}, K_{TAPE} and K_{CFRP} are the thermal conductivities of the EVA, ETFE, PET, TAPE and CFRP layers presented in Table 7.

The R_{CONVT} and R_{RADT} have been determined by the following equations

$$R_{CONVT} = \frac{1}{h_{CT}A} \tag{16}$$

$$R_{RADT} = \frac{1}{h_{rT}A} \tag{17}$$

The h_{CT} is the total convection heat transfer from the top surface. On the top surface, mixed convection occurs (Natural and Forced convection). So total heat transfer coefficient is the sum of the forced and natural convection heat transfer coefficients.

$$h_{CT} = h_{naturalC} + h_{ForcedC} \tag{18}$$

Now further forced convection heat transfer coefficient has been estimated from following correlation presented in Pavlovic et al. (2021).

$$Nu_{ForcedC} = \frac{h_{ForcedC}L}{k} = 0.13Re^{0.703}(1+\sin(\beta))^{0.38} \tag{19}$$

The natural convection heat transfer coefficient has been determined by the following correlation presented in Pavlovic et al. (2021).

$$Nu_{NaturalC} = \frac{h_{naturalc}L}{k} = 0.7386R_{aL}^{0.1826}(1+\cos(\beta))^{-0.4575} \tag{20}$$

Now radiation heat transfer coefficient from the top surface has been determined by following the equation presented in Singh & Yadav, 2022a; Chandel & Agarwal, 2017).

Table 7 Thermal properties of solar panel materials (Pavlovic et al., 2021)

Martials	Density (Kg/m^3)	Thermal conductivity (W/mk)	Specific heat capacity (J/kgK)
ETFE	1730	0.24	1172
EVA	945	0.35	2090
Silicon	2330	148	700
PET	1350	0.275	1275
CFRP	1490	6.83	1130
Tape	1012	0.19	2000

$$h_{rT} = \varepsilon_{ETFE}\sigma(T_{ETFE}+T_{atm})(T_{ETFE}^2+T_{atm}^2) \tag{21}$$

The convection and radiation thermal losses have been estimated the same way as from the top side. So the following correlation has been used in Vineet et al. (2023).

$$R_{CONVB} = \frac{1}{h_{CONVB}A} \tag{22}$$

$$R_{RADB} = \frac{1}{h_{RADB}A} \tag{23}$$

The heat transfer coefficient from side has been determined from following correlation (Tian et al., 2021).

$$h_{FB} = \frac{(90^\circ-\beta)}{90^\circ}h_{ForcedC} \tag{24}$$

$$Nu_{NaturalC} = \frac{h_{naturalB}L}{k} = 0.7386R_{aL}^{0.1826}(1+\cos(\beta))^{-0.4575} \tag{25}$$

So total heat transfer coefficient from the bottom of the solar panel is given by the following equation (Sanaye & Hajabdollahi, 2015).

$$h_{CONVB} = h_{FB} + h_{naturalB} \tag{26}$$

Now from bottom radiation heat transfer coefficient has been determined by following correlation (Elminshawy et al., 2019).

$$h_{rB} = \varepsilon_{CFRP}\sigma(T_{CFRP}+T_{atm})(T_{CFRP}^2+T_{atm}^2) \tag{27}$$

Exergy modelling

Figure 2d shows the schematic representation of the exergy balance on the solar air heater. The solar exergy reaches the solar panel which is the input exergy. Now, based on the properties of the solar panel material maximum exergy has been absorbed by the solar panel, and the remaining is reflected in the atmosphere. The absorbed exergy is converted into electric power and the remaining losses in the atmosphere. The exergy destruction inside the solar cell material is found out by the simple exergy balance on the solar panel system.

So the input exergy for the solar panel has been given by the following formula (Gürel et al., 2021; Laveyne et al., 2020).

$$E_{Xin} = SA\left[1-\left(\frac{4}{3}\right)\left(\frac{T_a}{T_{Sun}}\right)+\left(\frac{1}{3}\right)\left(\frac{T_a}{T_{Sun}}\right)^4\right] \tag{28}$$

The exergy reflected in the atmosphere is given by following the formula (Laveyne et al., 2020).

$$E_R = \left(1 - \frac{T_a}{T_m}\right) SAr \tag{29}$$

The exergy loss in the atmosphere is given by the following formula (Laseinde & Ramere, 2021).

$$E_{Loss} = \left(1 - \frac{T_a}{T_m}\right) Q_{Loss} \tag{30}$$

The loss in heat is determined by the formula.

The electric exergy is given by following formula (Alizadeh et al., 2018).

$$E_{Xel} = V_m I_m \tag{31}$$

The exergy destruction is given by following the formula

$$E_{Dest} = E_{Xin} - E_R - E_{Loss} - E_{Xel} \tag{32}$$

Now the exergy efficiency of the solar panel is given by following the formula

$$\varphi_{EX} = \frac{Exergy\ Recovered}{Exergy\ Supplied} \tag{33}$$

The final formula of exergy efficiency (Singh & Yadav, 2022a).

$$\varphi_{EX} = \frac{V_m I_m}{SA\left[1 - \left(\frac{4}{3}\right)\left(\frac{T_a}{T_{Sun}}\right) + \left(\frac{1}{3}\right)\left(\frac{T_a}{T_{Sun}}\right)^4\right]} \tag{34}$$

Optimization technique

The optimization techniques are used to determine the optimal solutions on which responses are maxima and minima or the area of interest. Several algorithms and techniques are available but their selection has been done based on the accuracy of the data. In this research Response Surface Methodology (RSM) technique has been used for determining the optimal solution of the input variables. The first time RSM was used by Box and Wilson in 1951. It is the collection of mathematical techniques which used the 2nd order model equations to represents the responses in terms of input variables. The 2nd order model equations have been generated by the data of input variables collected either by the experimental or the numerical methods. Figure 3 represents the process of working of RSM in MINITAB 17 software.

Furthermore, RSM is used to reduce of the experimental work by limited defined sets. These sets of input variables convert the experimental data into well-defined 2nd-order models of the responses. The 2nd order model equation is represented as follows.

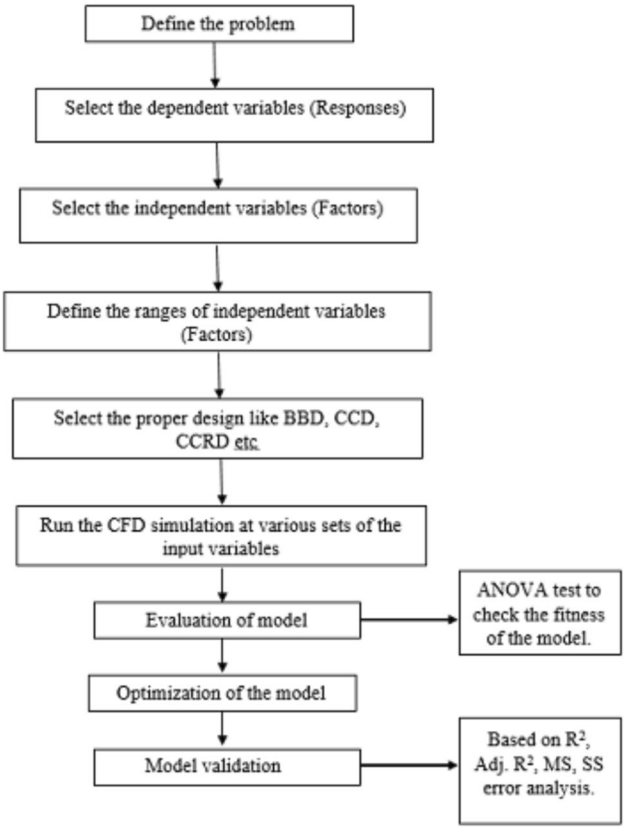

Fig. 3 Steps of process in RSM

Table 8 Ranges of the input variables

Input variables	Coded level		
	− 1	0	1
Solar flux (W/m^2)	600	800	1000
Air inlet velocity (m/s)	2	4	6
Atmospheric temperature (°C)	22	33	44

$$Y = A_\circ + \sum_{i=1}^{k} A_i x_i + \sum_{i=1}^{k} A_{ii} x_i^2 + \sum_{j\geq 1}^{k} A_{ij} x_i x_j + B \tag{35}$$

The xi and xj are the independent variables and Y is the response. A_0, A_i, A_{ii} and A_{ij} are the constants of the linear and square terms. The B represents the error or the noise in the model formation. Table 8 represents the range of the independent variables. The Box-Behenken design has been used for analysing the problem in which the total number of runs are 15 corresponding to the three input factors. Based on these 15 runs, the responses have been determined by simulation and model equation as shown in Table 9.

The effectiveness of the RSM has been judged by the R^2, adjR^2, P and F values of the Analysis of Variance (ANOVA)

Table 9 Total 15 runs of input and output variables

S. No.	Solar flux (W/m^2)	Atmospheric temperature (°C)	Velocity of air (m/s)	Solar cell temperature (°C)	Efficiency	Power output from solar panel (Wp)	Exergy efficiency
1	600	22	4	42	0.1631	41.3612	0.1741
2	600	33	6	48	0.1603	40.6518	0.1715
3	1000	33	6	63	0.1533	64.7972	0.1641
4	1000	22	4	60	0.1547	65.3884	0.1651
5	800	44	2	81	0.1449	49.0003	0.1555
6	800	22	2	62	0.1538	51.9954	0.1641
7	800	33	4	61	0.1542	52.1531	0.1651
8	800	44	6	66	0.1519	51.3649	0.1630
9	800	33	4	60.99	0.1542	52.1547	0.1651
10	600	44	4	62.34	0.1536	38.9564	0.1648
11	600	33	2	58.72	0.1553	39.3844	0.1662
12	800	33	4	61	0.1542	52.1531	0.1651
13	1000	44	4	79.82	0.1454	61.4829	0.1561
14	1000	33	2	82.212	0.1443	61.0115	0.1545
15	800	22	6	44.764	0.1618	54.7125	0.1727

presented in Tables 8, 9 and 10. The small value of P and larger values of F justified the effectiveness of the results (Tanwar et al., 2023). Table 10 represents the ANOVA table for the silicon cell temperature and the power output of the solar panel. Furthermore, it can be easily seen that most of the P values are lower than 0.05. The same results are also seen in Tables 11 and 12.

$$\begin{aligned} T_C = {} & 1.93 + 0.0777S + 0.723T_a \\ & - 4.865V - 0.000005S^2 + 0.00207T_a^2 \\ & + 0.5484V^2 - 0.000059ST_a \\ & - 0.005307SV + 0.0254T_aV \end{aligned} \tag{36}$$

Table 10 P-value and F value for checking the effectiveness of the regression analysis on cell temperature (Tc) and power output of solar panel (P)

Sources	DF	Silicon cell temperature (T_C)				Power output (P)			
		Adj. SS	Adj. MS	F-value	P-value	Adj. SS	Adj. MS	F-value	P-value
Model	9	2012.71	223.635	621.77	0.000	1101.38	122.38	7998.32	0.000
Linear	3	1975.03	658.343	1830.40	0.000	1098.37	366.12	23,929.50	0.000
S	1	683.98	683.982	1901.68	0.000	1065.52	1065.52	69,641.32	0.000
Ta	1	807.94	807.940	2246.32	0.000	20.01	20.01	1308.00	0.000
V	1	483.11	483.108	1343.19	0.000	12.84	12.84	839.16	0.000
Square	3	18.34	6.113	16.99	0.005	0.83	0.28	17.99	0.004
S*S	1	0.16	0.159	0.44	0.536	0.41	0.41	26.55	0.004
Ta*Ta	1	0.23	0.232	0.65	0.458	0.00	0.00	0.15	0.717
V*V	1	17.77	17.768	49.40	0.001	0.48	0.48	31.39	0.003
2–way interaction	3	19.35	6.449	17.93	0.004	2.18	0.73	47.48	0.000
S*Ta	1	0.07	0.068	0.19	0.683	0.56	0.56	36.80	0.002
S*V	1	18.03	18.029	50.12	0.001	1.59	1.59	103.62	0.000
Ta*V	1	1.25	1.250	3.48	0.121	0.03	0.03	2.30	0.214
Error	5	1.80	0.360	–	–	0.08	0.02	–	–
Lack of fit	3	1.80	0.599	17,982.92	0.000	0.08	0.03	30,784.03	0.000
Pure error	2	0.00	0.000	–	–	0.00	0.00	–	–
Total	14	2014.51	–	–	–	1101.45	–	–	–

Table 11 P-value and F value for checking the effectiveness of the regression analysis on efficiency of solar cell (η) and exergy entering to the solar panel (E_{Xin})

Sources	DF	Efficiency of solar panel (η)				Exergy entering (E_{Xin})			
		Adj. SS	Adj. MS	F-value	P-value	Adj. SS	Adj. MS	F-value	P-value
Model	9	0.000437	0.000049	621.77	0.000	1101.38	122.38	7998.32	0.000
Linear	3	0.000429	0.000143	1830.40	0.000	1098.37	366.12	23,929.50	0.000
S	1	0.000149	0.000149	1901.68	0.000	1065.52	1065.52	69,641.32	0.000
Ta	1	0.000176	0.000176	2246.32	0.000	20.01	20.01	1308.00	0.000
V	1	0.000105	0.000105	1343.19	0.000	12.84	12.84	839.16	0.000
Square	3	0.000004	0.000001	16.99	0.005	0.83	0.28	17.99	0.004
S*S	1	0.0000	0.000000	0.44	0.536	0.41	0.41	26.55	0.004
Ta*Ta	1	0.0000	0.000000	0.65	0.458	0.00	0.00	0.15	0.717
V*V	1	0.000004	0.000004	49.40	0.001	0.48	0.48	31.39	0.003
2–way interaction	3	0.000004	0.000001	17.93	0.004	2.18	0.73	47.48	0.000
S*Ta	1	0.0000	0.000000	0.19	0.683	0.56	0.56	36.80	0.002
S*V	1	0.000004	0.000004	50.12	0.001	1.59	1.59	103.62	0.000
Ta*V	1	0.0000	0.000000	3.48	0.121	0.03	0.03	2.30	0.214
Error	5	0.0000	0.000000	–	–	0.08	0.02	–	–
Lack of fit	3	0.0000	0.000000	17,982.92	0.000	0.08	0.03	30,784.03	0.000
Pure error	2	0.0000	0.000000	–	–	0.00	0.00	–	–
Total	14	0.000438	–	–	–	1101.45	–	–	–

Table 12 P-value and F-value for checking the effectiveness of the regression analysis of the exergy efficiency of solar panel

Sources	DF	Exergy efficiency (%)			
		Adj. SS	Adj. MS	F-value	P-value
Model	9	0.000466	0.000052	579.04	0.000
Linear	3	0.000457	0.000152	1702.23	0.000
S	1	0.000170	0.000170	1903.69	0.000
Ta	1	0.000166	0.000166	1858.63	0.000
V	1	0.000120	0.000120	1344.39	0.000
Square	3	0.000005	0.000002	17.04	0.005
S*S	1	0.000000	0.000000	0.44	0.536
Ta*Ta	1	0.000000	0.000000	0.78	0.417
V*V	1	0.000004	0.000004	49.46	0.001
2-way interaction	3	0.000005	0.000002	17.84	0.004
S*Ta	1	0.000000	0.000000	0.12	0.739
S*V	1	0.000004	0.000004	50.18	0.001
Ta*V	1	0.000000	0.000000	3.21	0.133
Error	5	0.000000	0.000000	–	–
Lack of fit	3	0.000000	0.000000	17,963.45	0.000
Pure error	2	0.000000	0.000000	–	–
Total	14	0.000466	–	–	–

$$\eta = 0.18176 - 0.000036S - 0.000337T_a + 0.002268V - 0.000001T_a^2 - 0.000256V^2 + 0.000002SV - 0.000012T_aV \quad (37)$$

$$P = 1.24 + 0.07030S + 0.0221T_a + 0.228V - 0.000008S^2 - 0.000204T_a^2 - 0.0902V^2 - 0.000171ST_a + 0.001574SV - 0.00401T_aV \quad (38)$$

$$E_{Xin} = 0.000062 + 0.398250S - 0.000004T_a - 0.000099ST_a \quad (39)$$

$$\eta_{EX} = 0.19297 - 0.000039S - 0.000310T_a + 0.002410V - 0.000001T_a^2 - 0.000274V^2 + 0.000003SV - 0.000012T_aV \quad (40)$$

Figure 4 represents the Pareto chart and the residual plot of the exergy efficiency predicted and actual results. Figure 4a clearly shows that solar flux, air inlet velocity, and the atmosphere temperature are most important parameters which affects the performance of the solar panel. Figure 4b clearly shows that most of the residual data lie within the range of ± 0.0002 which shows the validity of the model. Figure 4c depicts that data is fitted with an accuracy

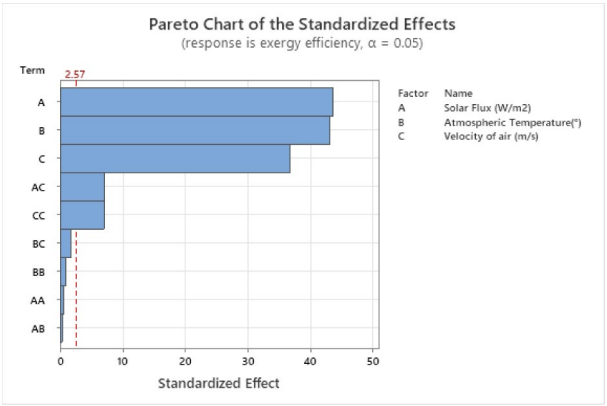

(a) Pareto Chart of Exergy efficiency

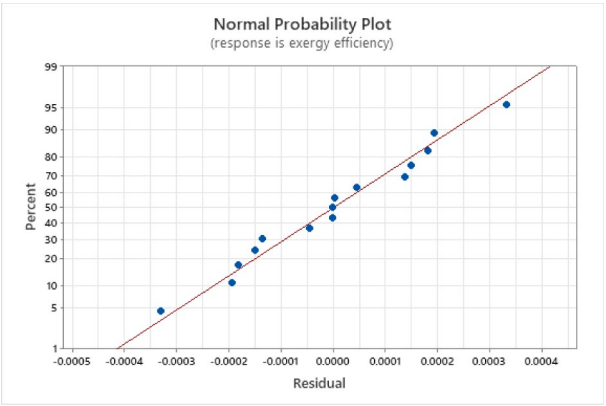

(b) Percent of residual of the exergy efficiency

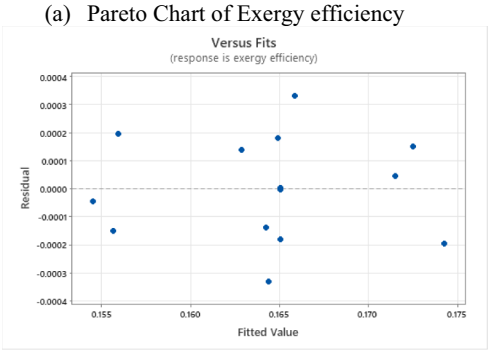

(c) Residual with the fitted values

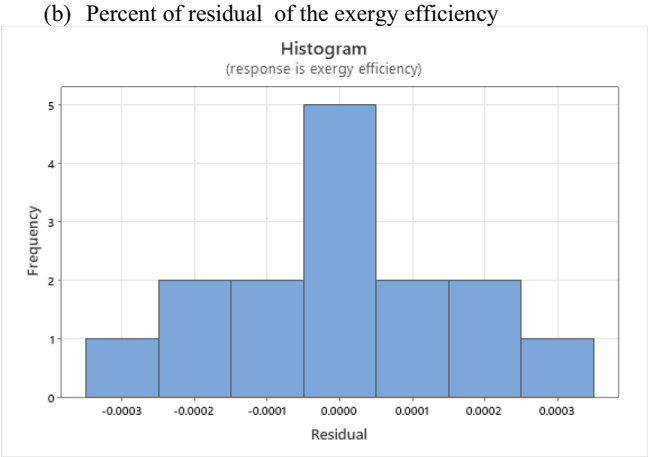

(d) Residual frequency with the residual

Fig. 4 Pareto and residual plot of the exergy efficiency of the solar panel

of ± 0.004. Figure 4d shows that the maximum frequency is represented by the 0 residual means most of the data point have the 0 residual.

Ansys modelling

The ANSYS 18.1 has been used to determine the solar panel's thermal analysis. The ANSYS workbench has the following steps for determining the temperature and solar flux plot presented in Fig. 5. Initially, the 3D model of the solar panel for the given dimensions was drawn in the geometry modeller as shown in Fig. 6a. The dimensions of the solar panel are 1153 mm × 513 mm and the thickness of various layers of the solar panel is given in Table 2 and Fig. 6b. Now, the geometry is discretized into the small control volume and this process is called the mesh generation.

The mesh generation is an important part of the Numerical Simulation since mesh quality affects the results and the conversance of the solution. Sometimes non uniform and unstructured mesh solutions will not converse. The total number of elements and nodes in Fig. 6c are 71,074 and 457,520. The skewness and orthogonality are two important parameters that defines the quality of the mesh. The skewness represents the actual meshes are how close to the ideal mesh and orthogonality represents the angular deviation of the actual mesh with the ideal mesh. In the Fig. 6c meshing, the average skewness and orthogonality of the meshing are the 0.0020246 and 0.99492 which represents the good quality of the mesh. Furthermore, each and every layer of the solar panel has been selected by different materials as presented in Tables 2 and 3. Now, boundary conditions have been applied based on the material properties of the layers of the solar panel. Now, finally, run the simulation and find the results from the post-processor.

Results and discussion

In the results and discussion section, the temperature and heat flux contour have been extracted from ANSYS Workbench at various solar flux, atmospheric temperature, and air flow velocity in Fig. 7. Furthermore, based on simulation data at various input parameters, the response is optimized

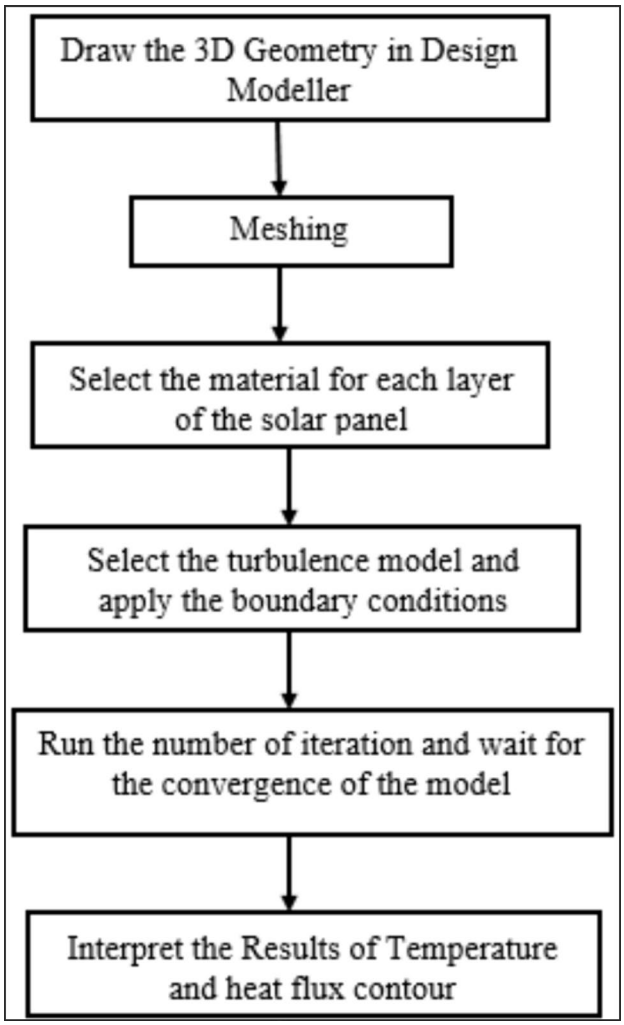

Fig. 5 Steps of the thermal analysis in ANSYS Workbench

by the Response Surface Methodology in MINITAB 17 software. The optimization results in the form of surface and contour plots have been represented in Figs. 8, 9, 10, 11, and 12.

Simulation results

Figure 7a–j represents the simulation results of the solar panel cooling at varying input conditions. Figure 7a and b represent the steady state temperature and solar flux plot at varying the 600 W/m^2, atmospheric temperature 22 °C, and air flow velocity 4 m/s. Figure 7a temperature contour plot shows that the maximum temperature is 41.924 °C in the middle cells of the solar panels and temperature reduces in outside of the solar panel. These simulation results depicted that the cooling should be provided at the middle of the solar panel. Figure 7b shows that the average total solar flux on the surface of the solar panel is 15,358 W/m^2. Figure 7c depicts that if the atmospheric temperature increase upto 33 °C at constant solar flux and air flow velocity, the maximum temperature increased from 41.92 to 47.953 °C. It shows that as the atmospheric temperature increases then the temperature of the solar panel also increased. Figure 7d also shows that if the atmospheric temperature enhanced then the solar flux on the solar panel reduced.

Figure 7e shows that if the solar flux increased to 1000 W/m^2 then the maximum temperature of the solar panel reached to 62.464 °C. It means that the enhancement in solar flux increased the module temperature. Figure 7f also shows that enhancement in solar flux enhanced the total heat flux upto 49,335 W/m^2. Figure 7g and h have represented the module temperature and heat flux at 1000 W/m^2 solar flux, 22 °C atmospheric temperature and 4 m/s air flow velocity. Figure 7g clearly shows that due to higher solar flux and lower atmosphere temperature, the maximum module temperature reached to be 60 °C. Figure 7h shows that the maximum heat flux reached to be 53,900 W/m^2 at the minimum area section of the solar panel. Figure 7i and j have drawn at higher atmospheric temperatures and lower air flow velocities. The higher atmospheric temperature and lower air flow velocity enhanced the solar panel temperature and total heat flux intensity as presented in Fig. 7i and f.

Variation of cell temperature with input variables

Figure 8 shows the variation of solar cell temperature with input variables namely air flow velocity, solar flux and the atmospheric temperature. Figure 8a and b depicted that if the airflow velocity increases then solar cell temperature reduces but if the solar flux and atmospheric temperature increase then the solar cell temperature increases (Singh et al., 2023), Fig. 8b contour plot depicted that higher solar flux and lower air inlet velocity enhanced the solar cell temperature out of the safe zone. Figure 8c and d also show that if the atmospheric temperature increases from 20 to 40 °C then the module temperature increases from 50 to 78 °C at a constant air velocity of 4 m/s (Elminshawy et al., 2019), which shows that atmospheric temperature promoted the cell temperature. Figure 8e and f displayed the variation of solar cell temperature with velocity of air and the atmospheric temperature at a constant solar flux of 800 W/m^2. The temperature of solar panel is less than 50 °C when the atmospheric temperature low and air velocity is high (Abdullah et al., 2021).

Variation of power output with input variables

Figure 9 represents the surface and contour plots of the solar panel's power output with the input variables. Figure 9a shows that as the atmosphere temperature increases, the power produced by the solar panel reduces at constant air velocity since an increase in atmosphere temperature enhances the solar cell temperature which reduces the power

Fig. 6 Ansys modeling of the solar panel

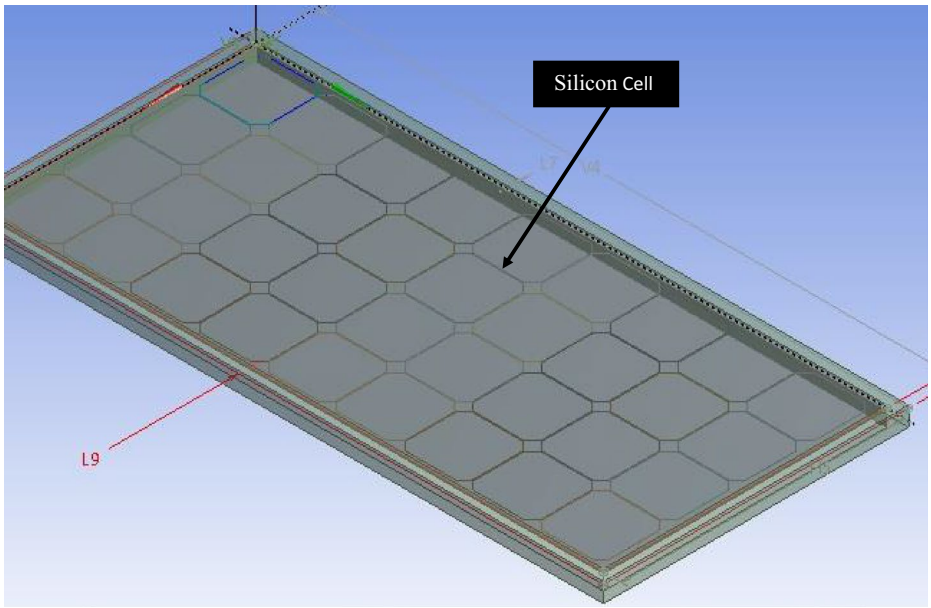

(a) CFD modelling in Ansys workbench 18.1

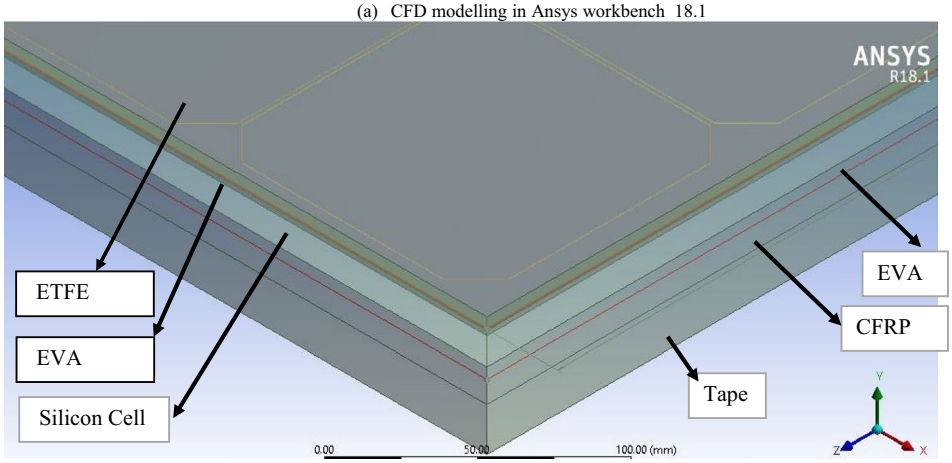

(b) Various layers in the solar panel

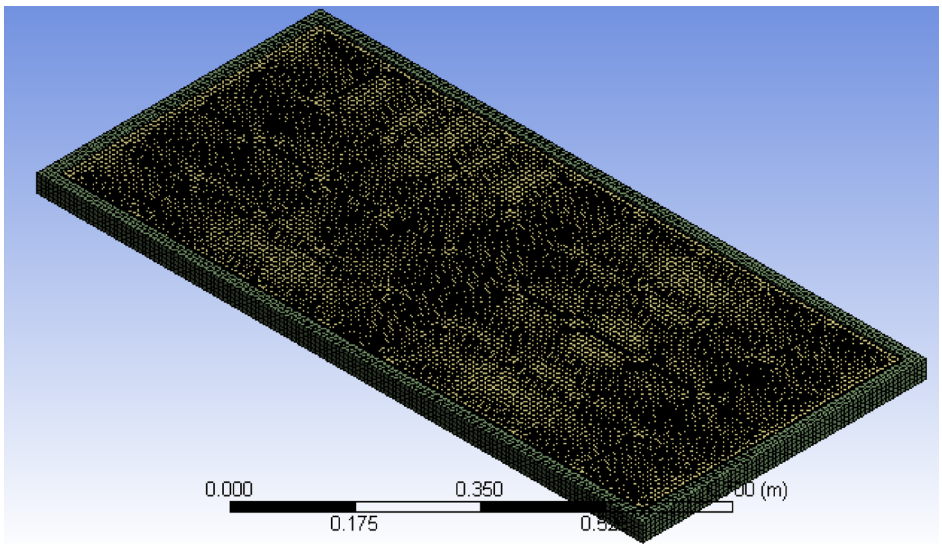

(c) Mesh generation in the solar panel

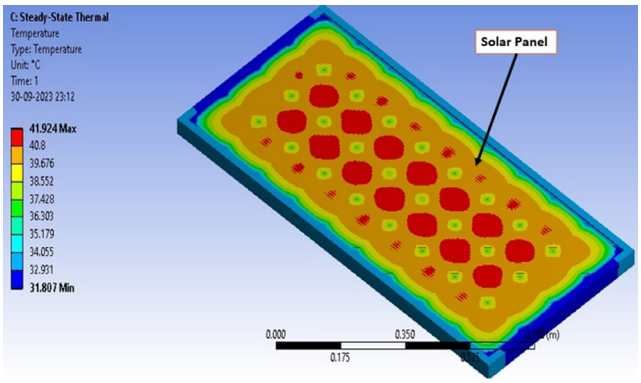

(a) Temperature of solar panel at S=600 W/m^2, Ta= 22°C, V= 4m/s

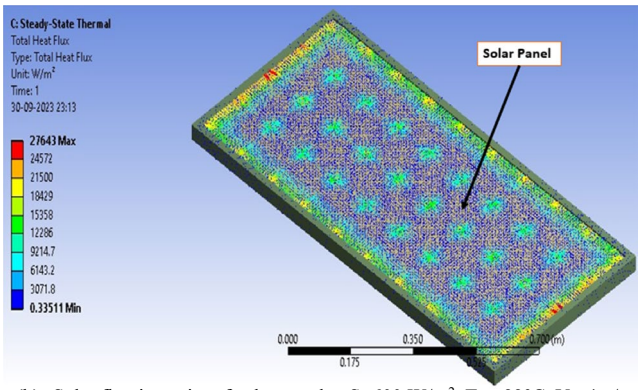

(b) Solar flux intensity of solar panel at S=600 W/m^2, Ta= 22°C, V= 4m/s

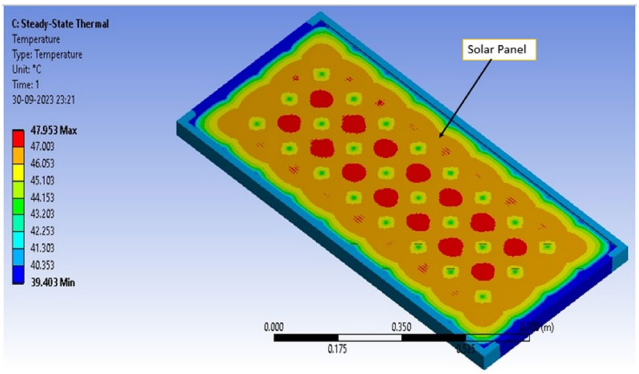

(c) Temperature of solar panel at S=600 W/m^2, Ta= 33°C, V= 6 m/s

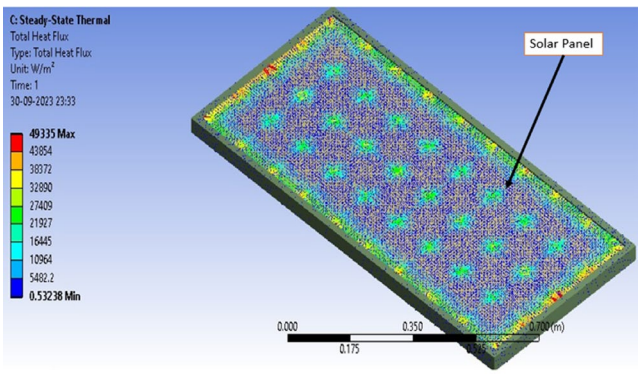

(d) Solar flux intensity of solar panel at S=600 W/m^2, Ta= 33°C, V= 6 m/s

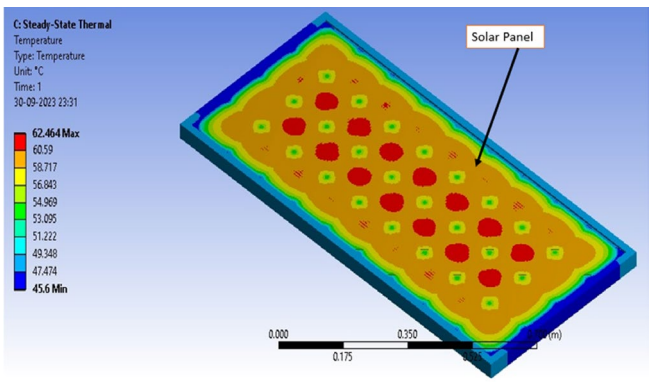

(e) Temperature of solar panel at S=1000 W/m^2, Ta= 33°C, V= 6 m/s

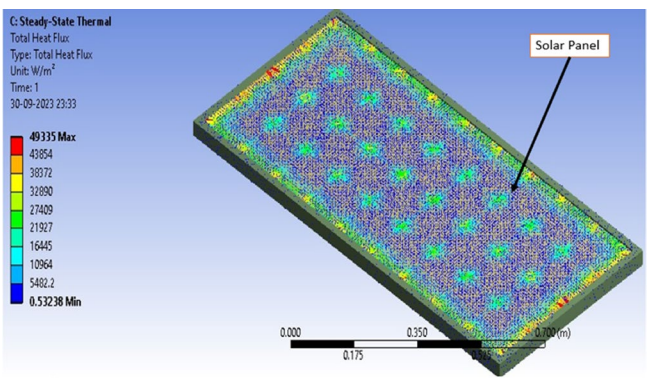

(f) Solar flux intensity of solar panel at S=1000 W/m^2, Ta= 33°C, V= 6 m/s

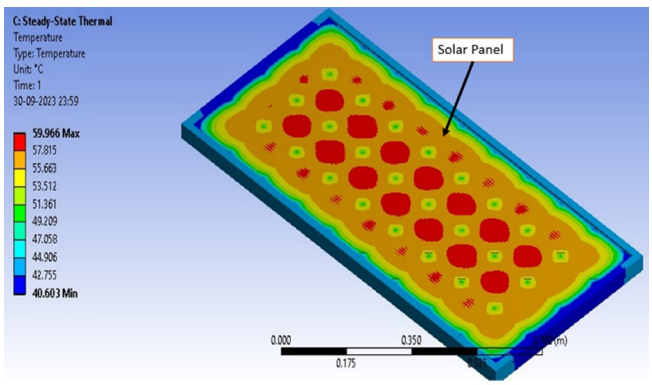

(g) Temperature of solar panel at S=1000 W/m^2, Ta= 22°C, V= 4 m/s

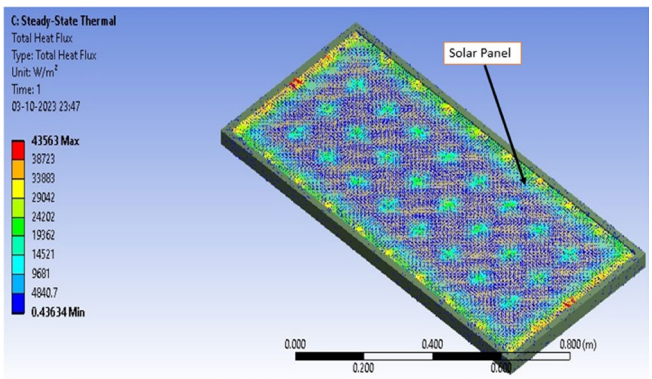

(h) Solar flux intensity of solar panel at S=1000 W/m^2, Ta= 22°C, V= 4 m/s

Fig. 7 Temperature and solar flux contour plot on solar panel

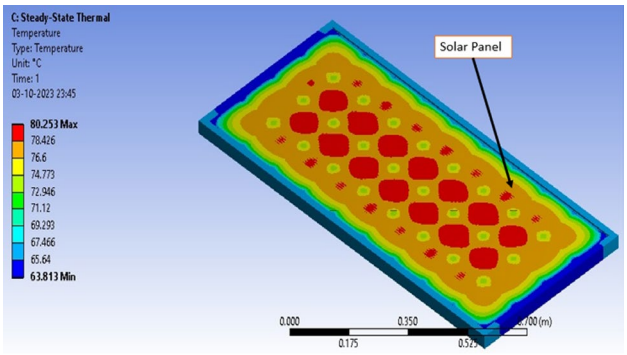

(i) Temperature of solar panel at S=800 W/m^2, Ta= 44°C, V= 2 m/s

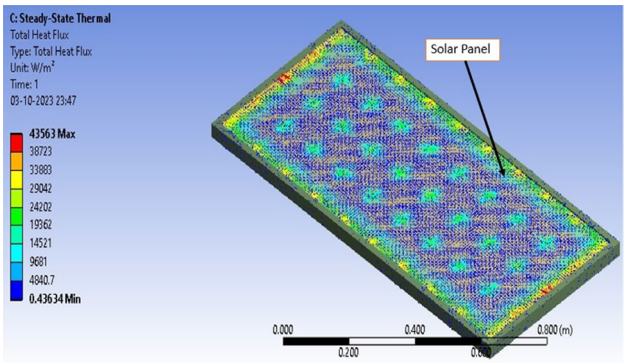

(j) Solar Flux intensity on solar panel at S=800 W/m^2, Ta= 44°C, V= 2 m/s

Fig. 7 (continued)

produced by the solar panel (Elminshawy et al., 2019). Figure 9b, the rightmost lower half part gives the maximum power output since higher solar flux supplies the higher solar energy to the solar panel, and lower atmospheric temperature maintains the lower solar cell temperature. Figure 9c shows that if the air velocity over the surface of the solar panel increases then the power produced by the solar panel increases since high air velocity increases the convection heat transfer coefficient (Mankani et al., 2022) since the heat transfer coefficient depends on the Reynolds number and fluid properties. The higher heat transfer coefficient enhances the heat transfer and maintains the temperature of the solar cell material within the safe limit. Figure 9d contour plot green region represents the power output of the solar panel more than 54.4 W at a constant solar flux of 800 W/m^2 (Salehi et al., 2021), this region is represents by the lower atmospheric temperature and higher air inlet velocity. Figure 9e shows that if the solar flux and air flow velocity increases then the power output increases since higher solar flux supplies more energy to the solar panel and higher air velocity maintains the cooling effect and lowers the cell temperature. Figure 9f contour plot topmost region represents the power output of the solar panel of more than 60 W. This region represents the higher solar flux and airflow velocity (Tiwari et al., 2020).

Variation of efficiency with input variables

Figure 10 represents the variation of solar panel efficiency with the input variables like solar flux, atmospheric temperature, and air velocity. Figure 10a shows that if the atmospheric temperature and solar flux both increases then the efficiency of the solar panel reduces since the increment in the atmospheric temperature reduces the heat loss in the atmosphere (Singh & Yadav, 2022a). Figure 10b dark green left corner region represents the maximum solar panel efficiency at lower atmospheric temperatures (Singh & Yadav, 2022b). Figure 10c shows that the enhancement in the air velocity increase the heat loss in the atmosphere which results in increased the efficiency of the solar panel. Figure 10d represents the contour plot of the efficiency of the solar panel with the air velocity and the solar flux. Figure 10e and f represent the 3 D and 2 D plots of the solar panel efficiency with the atmospheric temperature and the velocity of the air (Laseinde & Ramere, 2021). The enhancement in the airflow velocity increases the heat transfer to the air leads to reduction of the solar panel temperature (Salehi et al., 2021) and an enhancement of the solar panel efficiency.

Variation of exergy efficiency with input variables

Figure 11 shows the exergy variation of the solar panel with input variables. The chosen input variables are atmosphere temperature, solar flux, and air flow velocity. The Fig. 11a shows that as the solar flux increases, the exergy efficiency of the solar panel reduces since increased solar flux enhanced the temperature of solar panel cell material leads to reduction of the performance of the solar panel (Singh et al., 2023). Figure 11b shows that the maximum efficiency of the solar panel is 0.176 represented in the contour plot by the dark green region. In Fig. 11b dark green region is shown by the lower solar flux and atmospheric temperature region. Figure 11c surface plot clearly shows that if the air flow velocity increases from 2 to 6 m/s then the exergy efficiency of the solar panel also enhanced from 0.155 to 0.170. So, the 9.68% exergy efficiency of the solar panel increased due to incensement in air flow velocity (Amelia et al., 2016). The enhancement in the air flow velocity increases the heat transfer coefficient and air cooling (Govindasamy & Kumar, 2023). Figure 11d dark black part represents the maximum exergy efficiency of 0.170 at lower solar flux and higher air flow velocity. Figure 11e shows 3 D effect of the air

Fig. 8 Variation of cell temperature with input variables

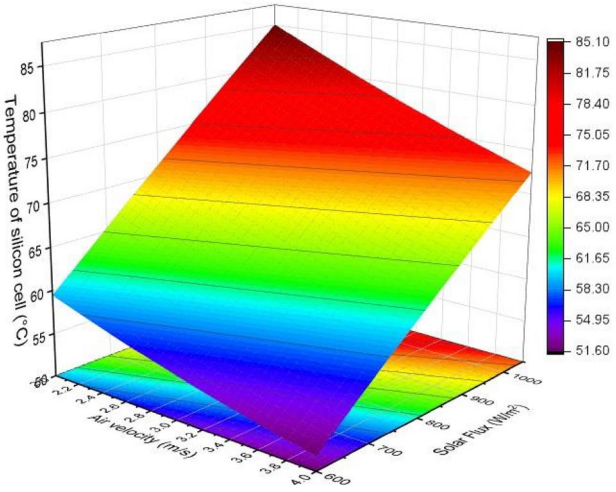

(a) Solar Cell temperature with air velocity and solar flux

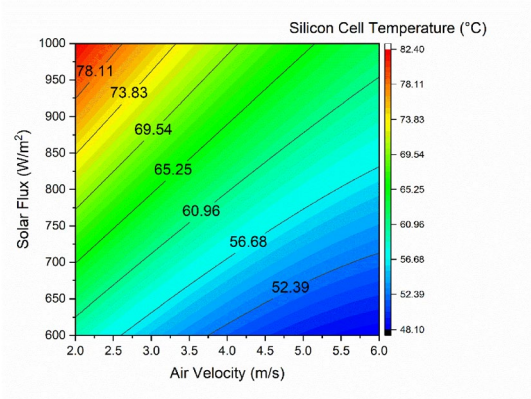

(b) Contour plot of solar cell temperature with air velocity and solar flux

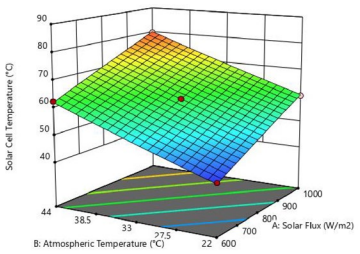

(C) Solar cell temperature with solar flux and atmospheric temperature

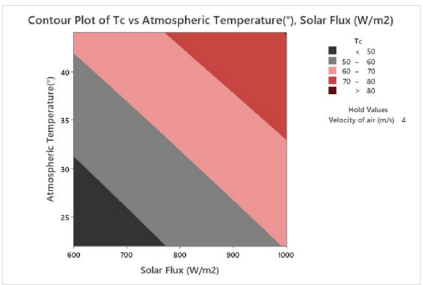

(d) Solar cell contour plot with solar flux and atmospheric temperature

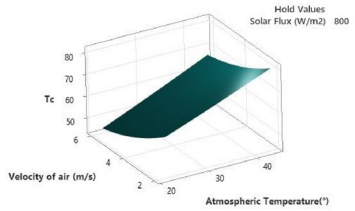

(e) Solar cell surface plot with air velocity and atmospheric temperature

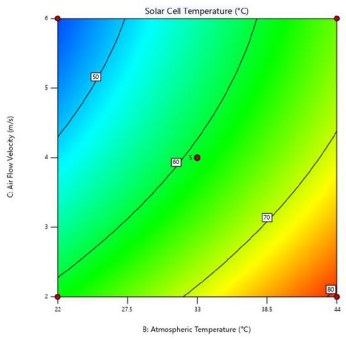

(f) contour plot of solar cell temperature with atmospheric temperature and air velocity

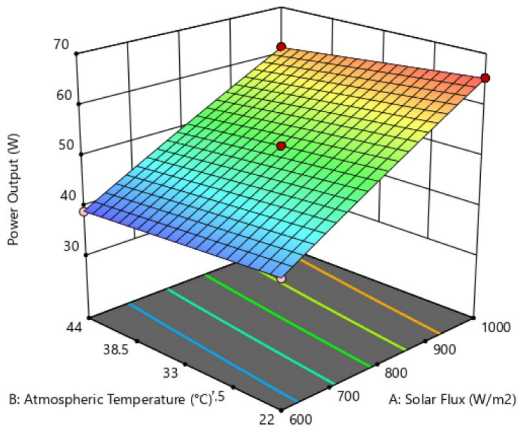

(a). Power output with the atmospheric temperature and solar flux

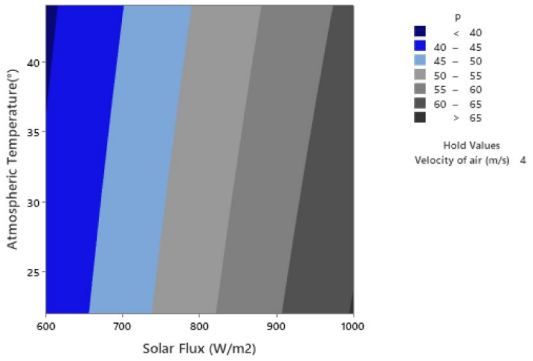

(b). Contour plot with atmospheric temperature and solar flux

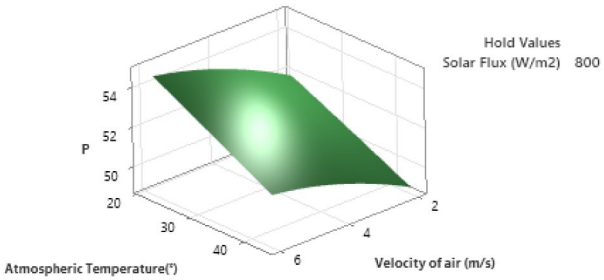

(c). Power output with the atmospheric temperature and air velocity

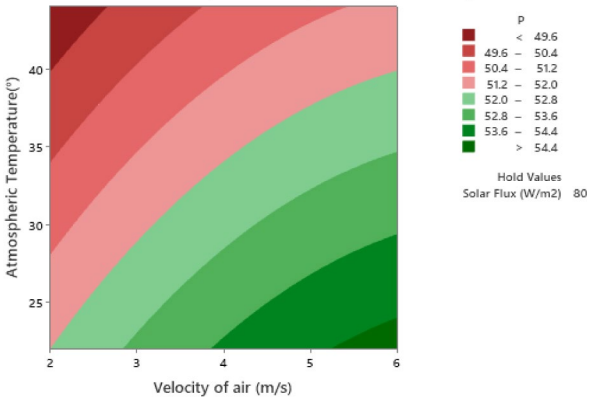

(d). Contour plot with atmospheric temperature and air velocity

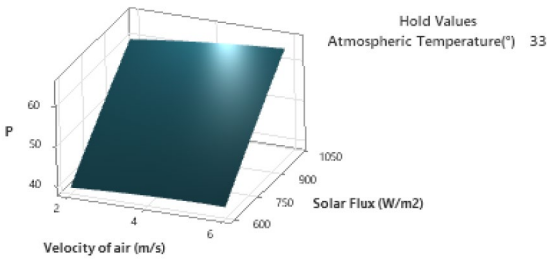

(e). Power output with the atmospheric temperature and air velocity

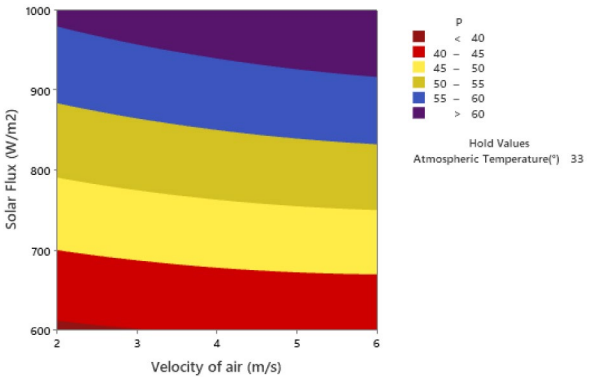

(f). Contour plot with atmospheric temperature and air velocity

Fig. 9 Variation of the power output of the solar panel with input variables

flow velocity and the atmospheric temperature on the exergy efficiency of the solar panel (Sultan et al., 1973). The figure clearly shows the steep variation of the air flow velocity on the solar panel exergy efficiency. Figure 11f dark red colour in 2 D plots represents the maximum exergy efficiency at lower atmospheric temperatures and higher air flow velocity (Mankani et al., 2022).

Optimization plot

Figure 12 represents the optimization plots of the output variables with respect to the input variables. The red-marked values in the plots show the optimum values of input and output variables. The optimum values of the input variables namely solar flux, atmospheric temperature, and velocity 974.3116 W/m^2, 22 °C and 6 m/s on which output

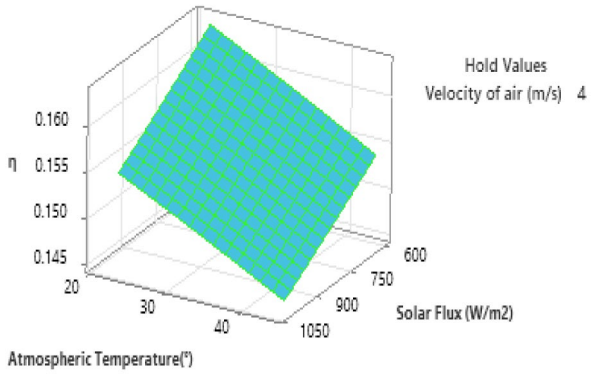

(a). Power output with the atmospheric temperature and solar flux

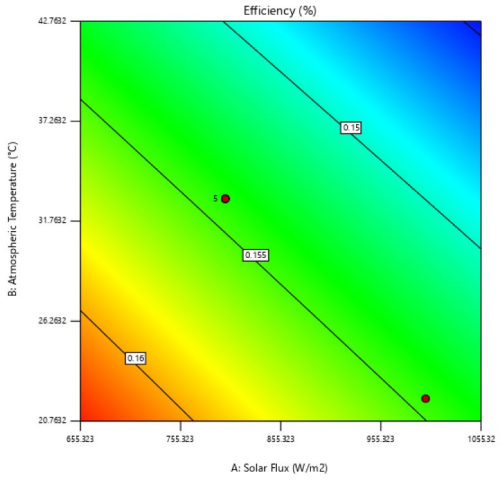

(b). Contour plot with atmospheric temperature and solar flux

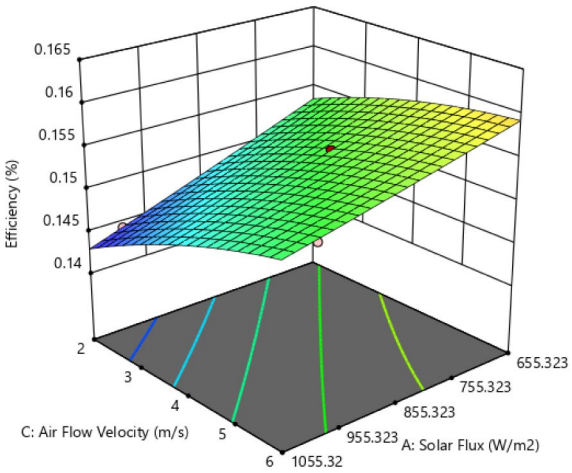

(c). Power output with the atmospheric temperature and air velocity

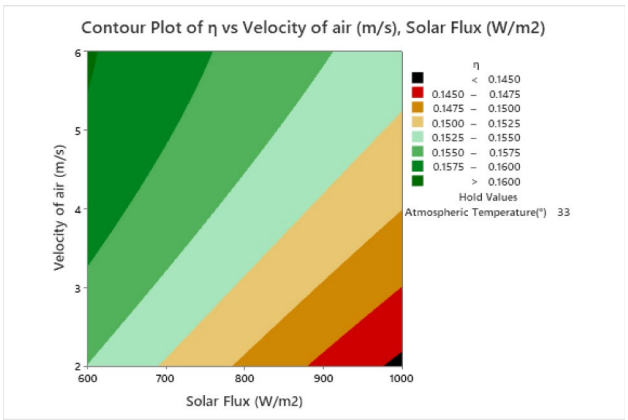

(d). Contour plot with atmospheric temperature and air velocity

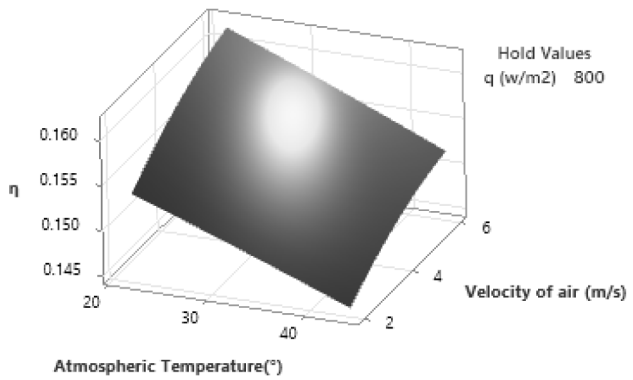

(e). Power output with the atmospheric temperature and air velocity

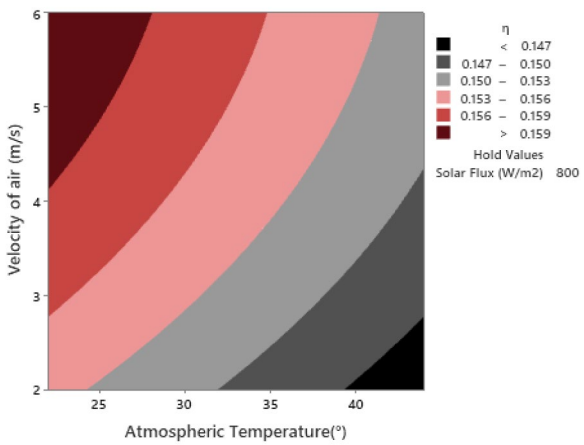

(f). Contour plot with atmospheric temperature and air velocity

Fig. 10 Efficiency of solar panel with input variables

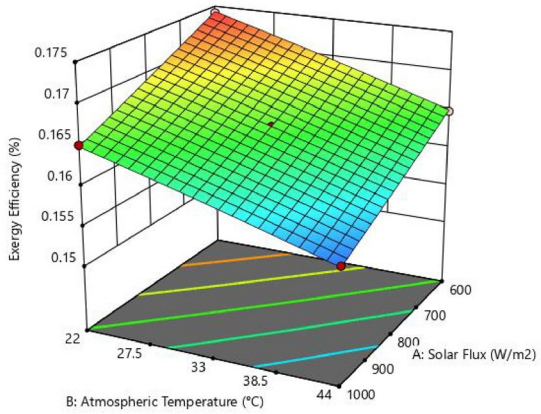

(a). Power output with the atmospheric temperature and solar flux

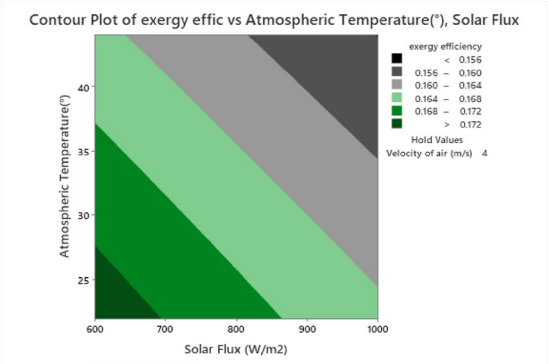

(b). Contour plot with atmospheric temperature and solar flux

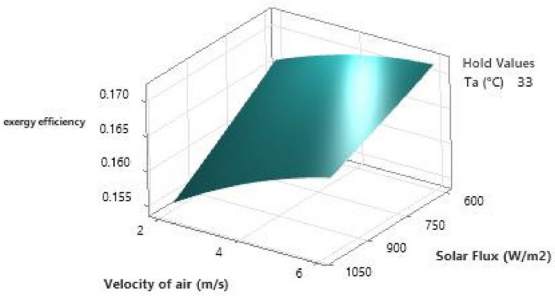

(c). Power output with the atmospheric temperature and air velocity

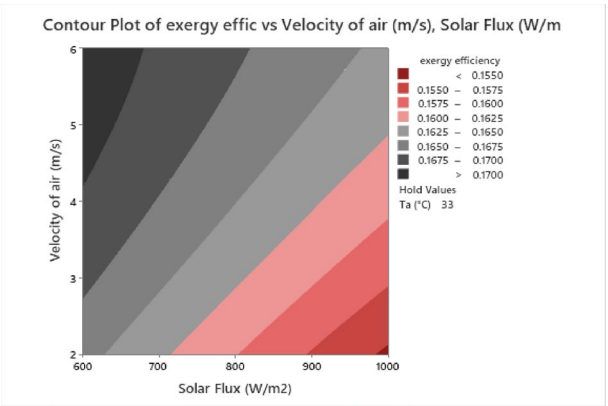

(d). Contour plot with atmospheric temperature and air velocity

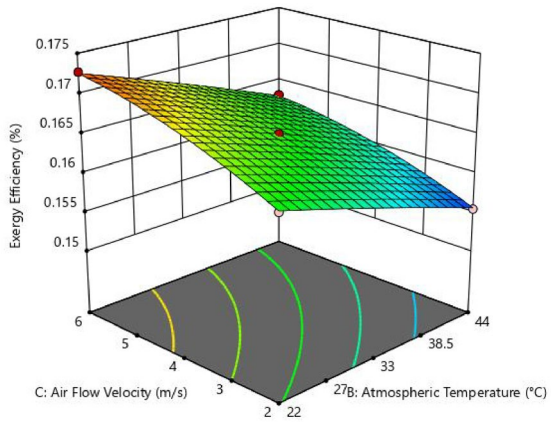

(e). Power output with the atmospheric temperature and air velocity

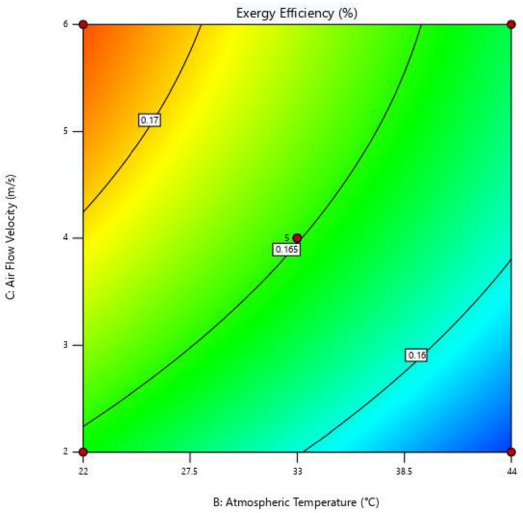

(f). Contour plot with atmospheric temperature and air velocity

Fig. 11 Exergy efficiency of solar panel with input variables

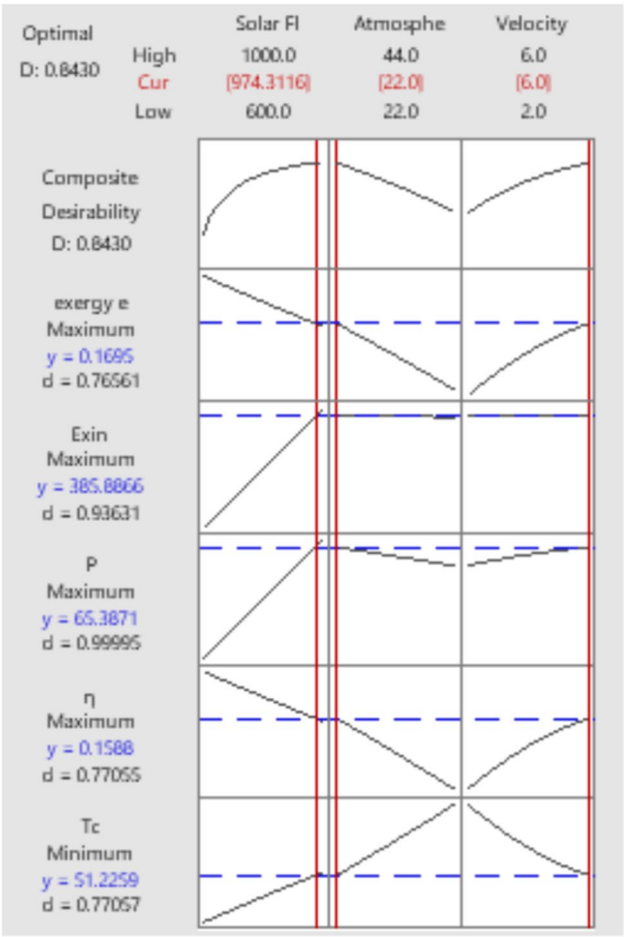

Fig. 12 Optimum plot of the input and output variables

variables like exergy efficiency, exergy supplied, power output, maximum efficiency, and module temperature are 0.1695, 385.886 W, 0.1588 and 51.2259 °C. The desirability represents the how well input variable affects the output variable (Singh Yadav et al., 2022). The combined desirability is 0.8430 and individual desirability of exergy efficiency, exergy entering into the solar panel, power out of solar panel, solar panel efficiency and cell temperature are 0.76, 0.93, 0.99, 0.77, and 0.77 respectively, which shows the good agreement between the input and output variables.

The optimum results show that the optimum atmosphere temperature is 22 °C, so the solar panel works better in the winter season than in other seasons.

Validation of the RSM results with experimental results

The optimum values of response parameters obtained by the RSM have been tested experimentally and validated. The RSM predicted results and experimental results with percentage error are represented in Table 13. Table 13 depicts that the percentage error in exergy efficiency, exergy entering the solar panel, the power output of the solar panel, solar panel efficiency, and solar cell temperature is 3.6, 4.2, 3.9, 2.8, and 4.5% respectively and well within the 5% that is acceptable.

Conclusion

In developing countries, solar panels have gained popularity in recent years due to the simple and easy conversion of solar energy into electric energy. The main problem with the solar panel is its low efficiency at higher temperatures. In a country like India, a number of studies depicted that the maximum temperature of the solar cell material reached around 70 to 80 °C in the summer season at 1 to 3 p.m. After crossing the nominal operating cell temperature (NOCT), the efficiency of the solar panel decreased. Many studies revealed that a 1 °C rise in temperature reduced the 0.5% solar panel efficiency (Peng et al., 2017; Yıldız et al., 2020). This study focuses on the simulation of the 100 Wp solar panel to determine the hot patches on the surface of the panel by contour plotting the temperature. Furthermore, the simulation data have been optimized by RSM in MINITAB 17 software for determining the best setting of the input parameters to maximize the performance of the solar panel. Finally, optimized results have been validated with the indoor experimental setup. Based on the above study, the following are the main concluding points.

Table 13 RSM and experimental results

	Exergy efficiency	Exergy entering to the solar panel (W)	Power of the solar panel (W)	Solar panel efficiency	Solar cell temperature (°C)
RSM forecast results	0.1695	385.886	65.3871	0.1588	51.2259
Experimental results	0.163398	369.6787	62.837	0.1543	48.920
% error	3.6	4.2	3.9	2.8	4.5

1. The thermal analysis simulation results show that the mid-section of the solar panel is the hottest as compared to other parts of the solar panel. So, most of the time cooling must be provided at the mid-section of the solar panel.
2. Simulation results, the 3D contour plot clearly shows that the solar flux and atmosphere temperature both increase the solar panel temperature and reduced the performance. The enhancement in air flow velocity enhances the heat transfer coefficient and performance of the solar panel.
3. The simulation results show that module temperature increased from 47.953 to 66.464 °C if the operating conditions of the simulation changed from S = 600 W/m^2, Ta = 33 °C, V = 6 m/s to S = 1000 W/m^2, Ta = 33 °C, V = 6.
4. At solar flux 800 W/m^2, atmospheric temperature 44 °C, and air inlet velocity 2 m/s, the solar panel temperature increased to 80.253 °C, which is the failure condition of the semiconductor material in the solar panel.
5. The optimum values of the solar flux, atmosphere temperature, and air flow velocity are 974.311 W/m^2, 22 °C and 6 m/s on which responses exergy efficiency 0.1695, exergy supply 385.88 W, power production 65.38 Wp, maximum efficiency of solar panel 0.1588 and minimum cell temperature 51.22 °C.
6. The desirability of the optimized results is 0.8430 which shows the good correlation between input and output variables in which solar flux and air flow velocity are main input variables which affect the performance of the solar panel.
7. The optimized results obtained by RSM have been tested experimentally and validated with an accuracy of 5%.
8. The Nominal Operating Cell Temperature (NOCT) of the solar cell material is 48.70 °C and the minimum cell temperature obtained by the optimization is 51.22 °C at solar flux 974.311 W/m^2, atmospheric temperature 22 °C and fan air velocity 6 m/s. If the solar panel module temperature works near the NOCT then it will give the good performance.

Solar plant and working principle

Solar plants based on solar panels are the best alternative to fossil fuels since fossil fuels are depleting nature and harnessing our environment. These plants convert solar energy directly into electricity at low maintenance and maintain durability for long life. The solar panels are made of solar cells which are made by semiconductor material. The semiconductor material has the conductivity between the metals and the insulator and due to that semiconductors are the very useful material (Tanwar et al., 2023). The conversion of the Sunlight into electricity is based on the photovoltaic conversion effect. When Sunlight falls on the solar cell, the free electron in the valence band absorbs the photon and moves the conduction band due to that the P–N junction generates a hole pair which will be separated further, and due to the flow of electrons (Yadav et al., 2021), the current will flow. The main problem with solar plants is their low efficiency at higher temperatures, the higher temperature of the solar panel material promotes the recombination losses and reduces the open circuit voltage of the solar panel. The reduction in voltage reduced the power output and efficiency of the solar panel (Shah & Mehta, 2021). This research numerical simulation and optimization technique show the optimum values of the air flow velocity at which the solar panel performance is maximum.

Acknowledgements The authors wish to thank all who assisted in conducting this work.

Declarations

Conflict of interest The authors want to affirm that there are no known conflicts of interest related to this publication.

Ethical approval This article does not contain any studies with human participants or animals performed by any of the authors.

References

Abdolzadeh, M., & Ameri, M. (2009). Improving the effectiveness of a photovoltaic water pumping system by spraying water over the front of photovoltaic cells. *Renewable Energy, 34*(1), 91–96. https://doi.org/10.1016/J.RENENE.2008.03.024

Abdullah, A. A., Attulla, F. S., Ahmed, O. K., & Algburi, S. (2022). Effect of cooling method on the performance of PV/Trombe wall: Experimental assessment. *Thermal Science and Engineering Progress, 30*(December), 101273. https://doi.org/10.1016/j.tsep.2022.101273

Alizadeh, H., Ghasempour, R., Shafii, M. B., Ahmadi, M. H., Yan, W. M., & Nazari, M. A. (2018). Numerical simulation of PV cooling by using single turn pulsating heat pipe. *International Journal of Heat and Mass Transfer, 127*, 203–208. https://doi.org/10.1016/J.IJHEATMASSTRANSFER.2018.06.108

Amelia, A. R., et al. (2016). Cooling on photovoltaic panel using forced air convection induced by DC Fan. *International Journal of Electrical and Computer Engineering, 6*(2), 526. https://doi.org/10.11591/ijece.v6i2.9118

Ceylan, İ, Gürel, A. E., Ergün, A., Guma Ali, İH., Ağbulut, Ü., & Yıldız, G. (2021). A detailed analysis of CPV/T solar air heater system with thermal energy storage: A novel winter season application. *Journal of Building Engineering*. https://doi.org/10.1016/j.jobe.2021.103097

Chaabane, M., Mhiri, H., & Bournot, P. (2016). Performance optimization of water-cooled concentrated photovoltaic system. *Heat Transfer Engineering, 37*(1), 76–81. https://doi.org/10.1080/01457632.2015.1042344

Chandel, S. S., & Agarwal, T. (2017). Review of cooling techniques using phase change materials for enhancing efficiency of photovoltaic power systems. *Renewable and Sustainable Energy Reviews, 73*(February), 1342–1351. https://doi.org/10.1016/j.rser.2017.02.001

Choi, S. M., Kwon, H. G., Kim, T., Moon, H. K., & Cho, H. H. (2022). Active cooling of photovoltaic (PV) cell by acoustic excitation in single-dimpled internal channel. *Applied Energy, 309*(November), 118466. https://doi.org/10.1016/j.apenergy.2021.118466

Dubey, S., Sandhu, G. S., & Tiwari, G. N. (2009). Analytical expression for electrical efficiency of PV/T hybrid air collector. *Applied Energy, 86*(5), 697–705. https://doi.org/10.1016/j.apenergy.2008.09.003

Ebaid, M. S. Y., Ghrair, A. M., & Al-Busoul, M. (2018). Experimental investigation of cooling photovoltaic (PV) panels using (TiO_2) nanofluid in water -polyethylene glycol mixture and (Al2O3) nanofluid in water- cetyltrimethylammonium bromide mixture. *Energy Conversion and Management, 155*(November), 324–343. https://doi.org/10.1016/j.enconman.2017.10.074

Elbreki, A. M., Sopian, K., Fazlizan, A., & Ibrahim, A. (2020). An innovative technique of passive cooling PV module using lapping fins and planner reflector. *Case Studies in Thermal Engineering, 19*, 100607. https://doi.org/10.1016/J.CSITE.2020.100607

Elminshawy, N. A. S., El Ghandour, M., Gad, H. M., El-Damhogi, D. G., El-Nahhas, K., & Addas, M. F. (2019). The performance of a buried heat exchanger system for PV panel cooling under elevated air temperatures. *Geothermics, 82*, 7–15. https://doi.org/10.1016/J.GEOTHERMICS.2019.05.012

Evola, G., & Marletta, L. (2014). Exergy and thermoeconomic optimization of a water-cooled glazed hybrid photovoltaic/thermal (PVT) collector. *Solar Energy, 107*, 12–25. https://doi.org/10.1016/J.SOLENER.2014.05.041

Fayaz, H., Nasrin, R., Rahim, N. A., & Hasanuzzaman, M. (2018). Energy and exergy analysis of the PVT system: Effect of nanofluid flow rate. *Solar Energy, 169*(May), 217–230. https://doi.org/10.1016/j.solener.2018.05.004

Govindasamy, D., & Kumar, A. (2023). Experimental analysis of solar panel efficiency improvement with composite phase change materials. *Renewable Energy, 212*(April), 175–184. https://doi.org/10.1016/j.renene.2023.05.028

Gürel, A. E., Yıldız, G., Ergün, A., & Ceylan, İ. (2021). Exergetic, economic and environmental analysis of temperature controlled solar air heater system. *Cleaner Engineering and Technology, 6*(April), 2022. https://doi.org/10.1016/j.clet.2021.100369

Hadipour, A., RajabiZargarabadi, M., & Rashidi, S. (2021). An efficient pulsed- spray water cooling system for photovoltaic panels: Experimental study and cost analysis. *Renewable Energy, 164*, 867–875. https://doi.org/10.1016/J.RENENE.2020.09.021

Hasan, A., McCormack, S. J., Huang, M. J., & Norton, B. (2014). Energy and cost saving of a photovoltaic-phase change materials (PV-PCM) System through temperature regulation and performance enhancement of photovoltaics. *Energies, 7*(3), 1318–1331. https://doi.org/10.3390/en7031318

He, W., Chow, T. T., Ji, J., Lu, J., Pei, G., & Chan, L. S. (2006). Hybrid photovoltaic and thermal solar-collector designed for natural circulation of water. *Applied Energy, 83*(3), 199–210. https://doi.org/10.1016/j.apenergy.2005.02.007

Jafari, R. (2021). Optimization and energy analysis of a novel geothermal heat exchanger for photovoltaic panel cooling. *Solar Energy, 226*, 122–133. https://doi.org/10.1016/J.SOLENER.2021.08.046

Kabeel, A. E., & Abdelgaied, M. (2019). Performance enhancement of a photovoltaic panel with reflectors and cooling coupled to a solar still with air injection. *Journal of Cleaner Production, 224*, 40–49. https://doi.org/10.1016/J.JCLEPRO.2019.03.199

Karami, N., & Rahimi, M. (2014). Heat transfer enhancement in a PV cell using boehmite nanofluid. *Energy Conversion and Management, 86*, 275–285.

Kumar, R., Deshmukh, V., & Bharj, R. S. (2020). Performance enhancement of photovoltaic modules by nanofluid cooling: A comprehensive review. *International Journal of Energy Research, 44*(8), 6149–6169. https://doi.org/10.1002/ER.5285

Laseinde, O. T., & Ramere, M. D. (2021). Efficiency improvement in polycrystalline solar panel using thermal control water spraying cooling. *Procedia Computer Science, 180*, 239–248. https://doi.org/10.1016/J.PROCS.2021.01.161

Laveyne, J. I., Bozalakov, D., Van Eetvelde, G., & Vandevelde, L. (2020). Impact of solar panel orientation on the integration of solar energy in low-voltage distribution grids. *International Journal of Photoenergy*. https://doi.org/10.1155/2020/2412780

Maleki, A., Ngo, P. T. T., & Shahrestani, M. I. (2020). Energy and exergy analysis of a PV module cooled by an active cooling approach. *Journal of Thermal Analysis and Calorimetry, 141*(6), 2475–2485. https://doi.org/10.1007/S10973-020-09916-0

Malvoni, M., Manoj, N., Chopra, S. S., & Hatziargyriou, N. (2020). Performance and degradation assessment of large scale grid-connected solar photovoltaic power plant in tropical semi-arid environment of India Performance and degradation assessment of large-scale grid-connected solar photovoltaic power plant in tropical. *Solar Energy, 203*(June), 101–113. https://doi.org/10.1016/j.solener.2020.04.011

Mankani, K., Nasarullah Chaudhry, H., & Kaiser Calautit, J. (2022). Optimization of an air-cooled heat sink for cooling of a solar photovoltaic panel: A computational study. *Energy and Buildings*. https://doi.org/10.1016/j.enbuild.2022.112274

Marudaipillai, S. K., Ramaraj, B. K., Kottala, R. K., & Lakshmanan, M. (2020). "Environmental effects experimental study on thermal management and performance improvement of solar PV panel cooling using form stable phase change material. *Energy Sources Part Recovery, Utilization, and Environmental Effects*. https://doi.org/10.1080/15567036.2020.1806409

Patil, M., Sidramappa, A., Hebbale, A. M., & Vishwanatha, J. S. (2023). Computational fluid dynamics (CFD) analysis of air-cooled solar photovoltaic (PV/T) panels. *Materials Today: Proceedings*. https://doi.org/10.1016/j.matpr.2023.05.198

Pavlovic, A., Fragassa, C., Bertoldi, M., & Mikhnych, V. (2021). Thermal behavior of monocrystalline silicon solar cells: A numerical and experimental investigation on the module encapsulation materials. *Journal of Applied and Computational Mechanics, 7*(3), 1847–1855. https://doi.org/10.22055/JACM.2021.37852.3101

Peng, Z., Herfatmanesh, M. R., & Liu, Y. (2017). Cooled solar PV panels for output energy efficiency optimisation. *Energy Conversion and Management, 150*, 949–955. https://doi.org/10.1016/J.ENCONMAN.2017.07.007

Revati, D., & Natarajan, E. (2016). Enhancing the efficiency of solar cell by air cooling. *Indian Journal of Science and Technology, 9*(5), 1–6. https://doi.org/10.17485/ijst/2016/v9i5/87274

Royne, A., & Dey, C. J. (2007). Design of a jet impingement cooling device for densely packed PV cells under high concentration. *Solar Energy, 81*(8), 1014–1024. https://doi.org/10.1016/j.solener.2006.11.015

Salehi, R., Jahanbakhshi, A., Golzarian, M. R., & Khojastehpour, M. (2021). Evaluation of solar panel cooling systems using anodized heat sink equipped with thermoelectric module through the parameters of temperature, power and efficiency. *Energy Conversion and Management: X*. https://doi.org/10.1016/J.ECMX.2021.100102

Sanaye, S., & Hajabdollahi, H. (2015). Thermo-economic optimization of solar CCHP using both genetic and particle swarm algorithms. *Journal of Solar Energy Engineering ASME*. https://doi.org/10.1115/1.4027932/379583

Shah, P., & Mehta, B. (2021). Mitigation of grid connected distributed solar photovoltaic fluctuations using battery energy storage station and microgrid. *International Journal of Power and Energy Conversion, 12*(2), 153–169. https://doi.org/10.1504/IJPEC.2021.114487

Shahverdian, M. H., et al. (2021). A dynamic multi-objective optimization procedure for water cooling of a photovoltaic module. *Sustainable Energy Technologies and Assessments*. https://doi.org/10.1016/J.SETA.2021.101111

Singh, B., et al. (2023). Performance improvement and optimisation using response surface methodology (central composite design) of solar photovoltaic module with reflector and automatic water cooling. *Process Integration and Optimization for Sustainability, 7*(1–2), 343–357. https://doi.org/10.1007/s41660-022-00296-6

Singh, V., & Yadav, V. S. (2022a). Optimizing the performance of solar panel cooling apparatus by application of response surface methodology. *Proceedings of the Institution of Mechanical Engineers, Part C*. https://doi.org/10.1177/09544062221101828.

Singh, V., & Yadav, V. S. (2022b). Application of RSM to optimize solar pump LCOE and power output. *IETE Journal of Research*. https://doi.org/10.1080/03772063.2022.2069165

Singh Yadav, V., Singh, V., Kumar, M., Kumar, N. (2022). Optimization and Validation of Solar Pump Performance by MATLAB Simulink and RSM, 九州大学グリーンテクノロジー研究教育センター バージョン: 権利関係: Evergr. Jt. J. Nov. Carbon Resour. Sci. Green Asia Strateg 9(4), 1110–1125, https://doi.org/10.5109/6625723

Sultan, T. N., Farhan, M. S., & Salim Alrikabi, H. T. H. (2021). Using cooling system for increasing the efficiency of solar cell. *Journal of Physics: Conference Series*. https://doi.org/10.1088/1742-6596/1973/1/012129

Tanwar, S. S., Dubey, R. K., & Prajapat, G. P. (2023). A multivariate regression model of solar photovoltaic and its validation through ANN. *International Journal of Power and Energy Conversion, 14*(4), 359–375. https://doi.org/10.1504/ijpec.2023.10060925

Teo, H. G., Lee, P. S., & Hawlader, M. N. A. (2012). An active cooling system for photovoltaic modules. *Applied Energy, 90*(1), 309–315. https://doi.org/10.1016/j.apenergy.2011.01.017

Tian, M. W., et al. (2021). Energy, exergy and economics study of a solar/thermal panel cooled by nanofluid. *Case Studies in Thermal Engineering, 28*, 101481. https://doi.org/10.1016/j.csite.2021.101481

Tiwari, A. K., Kumar, R., Pande, R. R., Sharma, S. K., & Kalamkar, V. R. (2020). Effect of forced convection cooling on performance of solar photovoltaic module in rooftop applications. *Advances in Energy Research*, *1*, 159–172. https://doi.org/10.1007/978-981-15-2666-4_16.

Tonui, J. K., & Tripanagnostopoulos, Y. (2008). Performance improvement of PV/T solar collectors with natural air flow operation. *Solar Energy, 82*, 1–12. https://doi.org/10.1016/j.solener.2007.06.004

Vineet Singh, A. B. B., Yadav, V. S., Bhutto, J. K., & Verma, R. (2023). Comparison of different designs of solar air heater with the simple solar heater of having reflecting mirrors. *Proceedings of the Institution of Mechanical Engineers Part C Journal of Mechanical Engineering Science*. https://doi.org/10.1177/09544062231158530

Wang, Y., Yu, L., Nazir, B., Zhang, L., & Rahmani, H. (2021). Innovative geothermal-based power and cooling cogeneration system; thermodynamic analysis and optimization. *Sustainable Energy Technologies and Assessments, 44*(December 2020), 101070. https://doi.org/10.1016/j.seta.2021.101070

Yadav, A., Deolia, V. K., & Agrawal, S. (2021). Indirect closed loop control of quasi-Z-source inverter for standalone solar PV-based energy conversion system. *International Journal of Power and Energy Conversion, 12*(3), 236–251. https://doi.org/10.1504/IJPEC.2021.116579

Yıldız, G., Çalış, B., Gürel, A. E., & Ceylan, İ. (2020). Investigation of life cycle CO_2 emissions of the polycrystalline and cadmium telluride PV panels. *Environmental Nanotechnology Monitoring & Management*. https://doi.org/10.1016/j.enmm.2020.100343

Yun, G. Y., Mcevoy, M., & Steemers, K. (2007). Design and overall energy performance of a ventilated photovoltaic facade. *Solar Energy, 81*, 383–394. https://doi.org/10.1016/j.solener.2006.06.016

Zakharchenko, R., et al. (2004). Photovoltaic solar panel for a hybrid PV/thermal system. *Solar Energy Materials and Solar Cells, 82*(1–2), 253–261. https://doi.org/10.1016/j.solmat.2004.01.022

Springer Nature or its licensor (e.g. a society or other partner) holds exclusive rights to this article under a publishing agreement with the author(s) or other rightsholder(s); author self-archiving of the accepted manuscript version of this article is solely governed by the terms of such publishing agreement and applicable law.